



MINISTRY OF TECHNOLOGY
AERONAUTICAL RESEARCH COUNCIL
CURRENT PAPERS

A Wind-Tunnel Investigation of the
Stalling Performance of Two Compressor Cascades
of Different Aspect Ratios at Low Speed

By

*M. R. A. Shaalan, B.Sc. Eng , Ph.D ,
Department of Mechanical Engineering,
The University of Liverpool*

LIBRARY
ROYAL AIRCRAFT ESTABLISHMENT

LONDON: HER MAJESTY'S STATIONERY OFFICE

1970

PRICE 10s 0d [50p] NET



AERONAUTICAL RESEARCH COUNCIL

March, 1968

TURBOMACHINERY SUB-COMMITTEE

A Wind-Tunnel Investigation of the Stalling Performance of Two Compressor Cascades of Different Aspect Ratios at Low Speed

- By -

M. R. A. Shaalan^{**}, B.Sc.(Eng.), Ph.D.,
Department of Mechanical Engineering,
The University of Liverpool

SUMMARY

Two compressor cascades of aspect ratio 2.10 and 4.83 were tested up to the stall point in a working section with solid side walls. A change in aspect ratio was obtained by changing the blade chord only. The blade section profile was the 10C4/30C50, staggered at 36 degrees with a space-chord ratio of 0.88, and there was no tip clearance. Reynolds number similarity was maintained but its value was kept above a "critical" value.

Substantial difference in performance is indicated between the two aspect ratios. The high aspect ratio cascade gives more deflection at the mid-span near stall, but stalls first. The long chord, low aspect ratio blade stalls gently whilst a classical type of sudden stall occurs at the other aspect ratio. Higher pressure rise coefficient is observed at the high aspect ratio, increasing slightly with incidence up to the stall point. Substantially higher spanwise contraction is evident with the low aspect ratio. The order of magnitude of the increase in axial velocity for both cascades is remarkably high.

Further tests show that the wall stall, which is present at each incidence, is different in the two cases. It appears that the flow near the wall in the long chord blade rotates further in the passage and the stall near the end wall is more along the blade than along the wall. In the case of the short chord, the separation areas along the blade and the wall are approximately equal.

The results for the overall performance are generally consistent with compressor work.

List/

* Replaces A.R.C.30 083

** Now lecturer in Mechanical Engineering, Ain Shams University, Cairo, UAR.

List of Contents

	<u>Page</u>
Summary	1
List of Contents	2
Notation	2
1. Introduction	4
2. Apparatus	5
3. Experimental Procedure and Investigation	6
4. Discussion	7
5. Conclusions	10
Acknowledgements	11
References	11

Notation

(a) Symbols

- A Blade aspect ratio (blade length/blade chord)
- AVR Axial velocity ratio (outlet axial velocity/inlet axial velocity)
- C Fluid velocity
- C_L Lift coefficient
- $C_p = \frac{P - P_1}{\frac{1}{2}\rho C_1^2}$ Local static pressure coefficient
- C_x Axial component of velocity
- C_y Tangential component of velocity
- $R_e = C_1 l / \nu$ Reynolds number
- $D = \frac{C_2}{C_{max}}$ Diffusion ratio
- h Blade length
- $i = \alpha - \alpha'$ Incidence angle
- K Calibration factor
- L Lift force

l	Blade chord length
P	Total pressure
p	Static pressure
s	Blade spacing
x'	Distance along chord measured from leading edge
y	Distance along cascade " " " "
z	Spanwise distance measured from end wall
α	Fluid angle (measured from cascade normal)
α	Blade angle (" " " ")
β	Stagger angle (" " " ")
ρ	Fluid density
$\delta = \alpha_2 - \alpha_2'$	Deviation (or boundary layer absolute thickness)
ν	Kinematic viscosity
$\Delta\alpha = \alpha_1 - \alpha_2$	Deflection (or turning angle)

(b) Subscripts

1	At inlet
2	At outlet
a	Atmospheric
m	Mean value
x	Axial
y	Tangential
TD	Two-dimensional
t	True
w	Wedge value
max	Maximum value
stall	Stall value

1. Introduction

Cascade data is still a reliable basis of compressor design. Through the cascade model, an indication is gained of the behaviour of the main design variables such as air outlet angles, losses, pressure rise, stall-free operating range, etc. Data obtained from systematic cascade testing is presented in the form of correlations covering a wide range of geometry and a variety of flow conditions. These conditions have been selected to simulate, roughly, those encountered in the real machine.

The compressor designer needs cascade information not only to select the profile that satisfies his design requirements, but also to check on the performance of the blade sections off-design. It is therefore essential that the blade element data covers a wide range of operation if the designer is to assess the overall characteristics of his stage.

The importance of the role of blade aspect ratio in determining the performance of an axial-flow compressor is well recognised. It has been shown that the overall characteristics of a compressor stage are adversely affected by increasing the aspect ratio and that severe wall stall is the primary cause of the deterioration in performance of high aspect ratio compressors. It has been suggested that the cause of wall stall must be found and eliminated if the performance of the high aspect ratio stage is to be improved.

The influence of aspect ratio on the performance of compressor cascades was first indicated in work by Erwin and Emery⁴. Their main conclusion was that the performance of cascades tested in a working section with porous side walls was unaffected by aspect ratio. But there was substantial evidence in Erwin and Emery's work that the performance of cascades of different aspect ratios was different when tested with solid side walls.

In compressor cascades - where the overall pressure gradient is adverse - the wall boundary layer is likely to separate in the corner bounded by the end wall and the blade suction surface provided the fluid turning angle is sufficient. Also, the boundary layer, when deflected, gives rise to secondary motion behind the cascade. The three-dimensional flow associated with the corner separation results in a strong stream contraction through the central part of the blade passage. None of these effects exists in a cascade tested in a working section where the wall boundary layer is extracted completely.

It is clear that further experimental studies are needed in which these effects can be clarified. Most tests on compressor cascades in which the aspect ratio was the only variable have been restricted to design point operation.

Carter² (1946), tested cascades having aspect ratio 1, 2 and 4 at design point. Carter studied the effect of variation in the entry velocity profile on the losses and concluded that as the profile got worse the loss peak moved towards the mid-span location. His general conclusion was that the total loss integrated over the whole blade height increased as the aspect ratio decreased and the losses were slightly influenced by changes in the velocity profile.

Rouffignac¹⁶ (1957) tested cascades having aspect ratios of 1.25 and 2.25: in all other aspects the geometry was similar. Inlet air velocity was fixed, so that Reynolds number similarity was not maintained. The low aspect ratio cascade produced higher stream contraction. A marked increase in deviation at the walls was evident at the higher aspect ratio; but this effect may be due to the low Reynolds number of the test in this case.

Horlock, Shaw, Pollard and Lewkowicz¹⁰ (1964), in their study of the effect of Reynolds number of cascade performance, tested cascades having aspect ratio 2, 3, 4 and 4.83. The high aspect ratio cascades (3.0), showed a marked increase in deviation when Reynolds number was reduced below a "critical" value (1.0×10^5). The low aspect ratio cascade showed little change in performance at such low Reynolds number. Pollard¹³ (1964) also concluded that the centreline performance was unaffected by secondary flow developed near the walls for aspect ratios ≥ 3.0 . He suggests that axial velocity ratio and the aspect ratio are important parameters in determining the stall point.

It was seen from this short review that the performance of compressor cascades of different aspect ratios taken up to the stall point remained to be investigated. This constituted the subject of the work reported here.

2. Apparatus

(a) The wind tunnel

The solid side wall blower tunnel No. 2 of the Mechanical Engineering Department, Liverpool University, was used for the present investigation. Modifications of the working section and the traversing equipment were introduced. The mechanism for incidence varying is shown schematically in Fig.1.

(b) The cascades

Two geometrically identical cascades of profile 10C4/30C50 were built: one of aspect ratio 2.10 and the other of aspect ratio 4.83. In order to maintain the ratio of the boundary layer thickness to the blade length, and thus reduce the number of variables, it was necessary to change the blade chord only, for a change in aspect ratio.

The determination of the chord length was governed by (i) the dimensions of the existing working section, (ii) the space-chord ratio selected (0.875), and, (iii) the practical minimum number of blades in cascade, (see Ref. 18). The geometry of the experimental cascades is summarised by the following table:

	A = 2.10	A = 4.83
Profile	10C4/30C50	10C4/30C50
Space/chord	0.87	0.89
Stagger (deg)	36	36
α_1' and α_2' (")	51 and 21	51 and 21
Chord length (in.)	13.80	6
Span (inches)	29	29

The blades were made of resin reinforced with fibre glass in the form of "chop stranded matting". The method of manufacture is described in detail in Ref. 17. Excellent surface finish was obtained and warpage and shrinkage effects were negligible. The blade profile was checked following a procedure which is described by Gostelow⁷. Fig. 2 shows the experimental cascades.

(c) The traversing mechanisms

The cascade tunnel was provided with facilities for traversing the flow at entry to and exit from the cascade. Spanwise as well as tangential traversing in a plane at one chord length distance from the leading edge plane was possible in the upstream region. In the downstream region traversing in the three mutually perpendicular directions was possible using a universal type of traversing mechanism.

(d) Instrumentation and calibration

The preliminary experiments in the early stages of the present work were carried out using a claw-type probe assuming that the static pressure downstream was atmospheric. Later on, the validity of this assumption became doubtful and the need to measure the outlet static pressure grew when it was decided to use a wedge-type instrument.

The wedge instrument was calibrated against a standard NPL probe which was assumed to give true readings for total and static pressure. The calibration experiment was conducted over a range of Reynolds number corresponding to air speeds from 25 ft/sec to 70 ft/sec and at a turbulence level which was much the same as that of the actual tests (0.30%). The dynamic head calibration factor is defined as:

$$K = \frac{P_t - p_t}{P_w - p_w}$$

where P_t : total head from NPL probe (true)
 p_t : static head from " " (")
 P_w : total head from wedge probe (true)
 p_w : static head " " " (false)

A sample of calibration results is given in Fig. 3.

The probe in question was also calibrated for yaw against a claw-type probe. From the calibration a reading was established on the protractor and to which all subsequent angle readings were referred.

3. Experimental Procedure and Investigation

3.1 Experimental procedure

At the beginning of each experiment, it was essential to attain reasonably uniform conditions at entry to the cascade. This was obtained by means of adjusting both top and bottom suction rates and, also, the included angle of the bottom diffuser. (See Fig. 1).

Given/

Given low free-stream turbulence intensity, sufficiently low values of Reynolds number give rise to laminar separation over most of the blade suction surface. This separation may occur at low incidence resulting in high loss. Horlock, Shaw, Pallard and Lewkowicz¹⁰ have shown that there is a minimum value of Reynolds number to have no effect on the performance - a conclusion which was reached also by Rhoden¹⁵. This "critical value" is about 1.0×10^5 for the cascade under investigation. Reynolds number value in the present work was varied from 1.2×10^5 to 3.5×10^5 .

3.2 Investigation

The mid-span performance of cascades of different aspect ratios was first examined. When significant differences in performance became evident, further tests were conducted in an attempt to explain the differences. In this respect, surveys of total, static pressure and flow angle were made extending from the mid-span location to the end wall and covering one blade pitch. Sets of pressure distribution were recorded, not only at centreline, but also at off-centreline locations gradually approaching the side wall.

Details of the investigation may best be presented by the following table:

Test	Location (inches from wall)	$\phi = 90 - \alpha_1$ Degrees	R_e	Results on Fig. Nos.
Mid-section performance	$14\frac{1}{2}$	37 -- 26	1.2×10^5 -- 3.5×10^5	(4) -- (7)
Profile Pressure Distribution	$14\frac{1}{2}$	37 -- 26	1.2×10^5 -- 3.5×10^5	(15) -- (20)
	$14\frac{1}{2}$ -- 1	37 and 30	2.0×10^5	(21) -- (24)
Area - traverses	$14\frac{1}{2}$ -- $\frac{1}{2}$	37 and 30	2.0×10^5	(8) -- (11)

ϕ : Cascade angle to the horizontal direction (see Fig. 1).

4. Discussion*

4.1 The overall centreline performance

The most interesting result is the variation of fluid deflection with incidence which is shown by Fig. 4a. Whilst there is virtually no difference in deflection between the two cascades near design, the deflection from the higher aspect ratio is markedly higher at near-stall operation. A classical type of abrupt stall is exhibited by cascade 5,

the/

* For convenience throughout the discussion, cascade of aspect ratio 4.83 and cascade of aspect ratio 2.10 will be labelled Cascade 5 and Cascade 2 respectively.

the type that had been observed by Howell¹¹ and others. Cascade 2 (which has not been tested by Howell) stalls gently. On the other hand, stalling of the higher aspect ratio is seen to have taken place at an incidence some 3 degrees less. The negligible effect of Reynolds number on the result may be seen from the plot.

The variation of the non-dimensional pressure rise produced by the cascade is given by Fig. 4b. Both curves indicate but slight variation in the pressure coefficient over the incidence range. However, the two results are significantly different. The reason for this will be made clear later.

The corresponding variation of the fluid outlet angle with incidence together with the total pressure loss are given by Figs. 5a and 5b. Losses at cascade 5 suddenly rise at stall to about 16% of the inlet dynamic head. A gradual increase in the loss coefficient is shown by the low aspect ratio cascade.

From measurements before and aft of the cascade, the centreline pitch-averaged axial velocities were derived. The axial velocity ratio ($AVR = \frac{\bar{C}_{x_2}}{\bar{C}_{x_1}}$) was plotted versus the ratio $(\cos \alpha_1 / \cos \alpha_2)$. If the AVR is taken as a measure of the amount of fluid contraction, then it may be seen from Fig. 6 that the flow contracts more at the low aspect ratio. The order of magnitude of the contraction for both aspect ratios is strikingly high (1.30 - 1.40). The result for cascade 5 is in almost exact agreement with that obtained by Rhoden¹⁵ for aspect ratio 3 but with unity space-chord ratio. Another important result, seen from the contraction curve, is the sudden reversal of the curve at stall, for cascade 5. This is associated with the sharp increase in the total pressure loss of Fig. 5b and the outlet angle of Fig. 5a. Cascade 2 shows a continuing increase in contraction - which is consistent with the loss and outlet angle variation observed. Rhoden's results do not show a reversal on the contraction, probably because he had not stalled his cascade completely.

4.2 "Wall stall"

Wall stall in compressor cascades has been observed by many research workers. It is a result of the interaction of the wall and the profile boundary layers in the region bounded by the "end-wall" and the blade suction surface. The presence of rotation, caused by the secondary vorticity resulting from the deflection of the wall boundary layer, causes the separation region to propagate along the blade towards the centreline and the separation is partly along the wall and partly along the blade. The relative extent of the separation zone on the wall and the blade depends on the adverse pressure gradient and the severity of the secondary vorticity leading to the rotation of the fluid in the blade passage near the end wall.

Wall stall was also observed by the present author. Figs. 8 - 11 show the total pressure contours behind the cascade, indicating a region of zero flow in the corner. The measurements were accompanied by severe unsteadiness in that region. The flow was completely tangential ($\alpha_2 = 90^\circ$) - the type of flow that had been observed by Horlock⁸ and which was comprehensively investigated by Armstrong¹. The rotation of the total pressure contours is also evident. Considerable growth of the separation zone with incidence is seen from the plots. It may be seen also that while wall separation is present, there is no sign of two-dimensional stall at the mid-span even at a high incidence. Figs. 21 - 24 showing the profile pressure distribution at spanwise locations close to the end wall prove the existence of partial separation on the blade suction surface in the corner region.

Wall stall also modifies the outlet angle from a compressor cascade and gives rise to the disparity that occurs between predictions from secondary flow theories and experiment. Horlock⁸, Horlock, Percival, Louis and Lakshminarayana⁹, and Armstrong¹ have shown that the maximum variation in outlet angle from a compressor cascade occurs at more than twice the entry boundary layer thickness from the end-wall. This result is confirmed in Figs. 14 and 15.

4.3 Increase in axial velocity

The principal effect of wall stall is the destruction of the two-dimensionality of the mainstream and the consequent increase in axial velocity. The effect of the enormous increase in axial velocity observed on the pressure rise may be seen from Fig. 25. In this figure the inlet dynamic head available for pressure rise has been broken down to various components. It is clear that the increase in axial velocity is the predominant cause of the deterioration of the static pressure rise coefficient. The effect of total pressure losses is small until close to stall, when it becomes dominant.

4.4 Total pressure contours

In order to further explain the different performance, detailed investigation behind the cascade was carried out. Figs. 8 - 11 show contours of non-dimensionalised total pressure relative to the atmospheric condition, and indicate a difference in the flow pattern behind the cascade. It may be seen by comparing the plots that the nature of the end-wall stall is different. The longer chord blade (lower aspect ratio) shows a separation region which extends more along the blade than along the wall. This is a secondary flow effect, since, with the longer channel, the flow has time to rotate further. For the low chord (high aspect ratio) the separation areas on the end-wall and suction surface are approximately equal. Further, the separation area is bigger for the lower chord and there is bigger contraction through the mid-span (see Fig. 6). This difference in the flow pattern explains the different performance which has been discussed. The difference in the fluid contraction is responsible for the difference in the pressure rise prior to stall. The stall mechanism determines the behaviour of the performance thereafter. The considerable movement of the end-wall stall towards the centreline explains the gradual stall of the low aspect ratio. The continuing increase in axial velocity shown by the low aspect ratio cascade (Fig. 6) means that the wake blockage stays unimportant compared to the wall stall in this case. In the other case ($A = 4.83$), the wall stall becomes unimportant at "mainstream" stall when the wake blockage has become so large that both the deviation and the total pressure losses increase sharply and the axial velocity ratio falls consequently. Again, this effect may be attributed to secondary flow. Not only is the secondary flow more severe for the low aspect ratio but also because there is more freedom for rotation its effect is transmitted further along the blade. This result is seen from Figs. 14 - 15, where the underturning has its peak at about twice the entry boundary layer thickness from the wall for cascade 5 whilst the peak occurs at more than three times the same thickness from the wall in the case of cascade 2. The earlier stall of cascade 5 may be explained as due to the higher adverse pressure gradient associated with the smaller contraction.

4.5 Profile pressure distribution

Several sets of pressure distributions were recorded for both cascades. The better unstalled performance of cascade 5 is evident from Figs. 16 and 17. The effect of the difference in axial velocity ratio is also seen in these plots, being pronounced near stall. Comparison of the

pressure distribution at sufficiently high incidence (Fig. 18) (when cascade 5 has already stalled) shows the marked deterioration in the pressure distribution on the rear half of the suction side of the high aspect ratio blade. Although the axial velocity ratio is much lower in this case, the separation of the boundary layer on the suction side is so severe that the pressure curve has flattened completely near the trailing edge.

Figs 21 - 24 show plots of pressure distribution recorded at each aspect ratio for off-centrelines locations and they correspond to the total pressure contours of Figs. 8 - 11. The deterioration of the lift coefficient near the wall is evident. These results also confirm the conclusions from the total pressure contours in that they indicate the blade stall near the blade end which is induced by the slow moving fluid in the corner region.

4.6 Comparison with compressor results

The performance of axial flow compressors has been shown to be adversely affected by increase in the blade aspect ratio. High aspect ratio compressors generally have steep characteristics, whereas low aspect ratio compressors have a wider range of unstalled operation. There is general agreement between this result and the cascade result given here, in which a large incidence range is observed. However, the characteristics of low aspect ratio compressors show higher pressure rise. This is probably due to a marked drop in the total pressure loss with decrease in the aspect ratio in the case of the compressor. It is the total pressure loss rather than the increase in axial velocity that is thought to be playing an important role in affecting the compressor characteristics. This argument is based on results by Fahmi², who tested two low speed compressors of aspect ratio 1 and 2. However, it should be noted that Fahmi's higher aspect ratio is the present author's lower.

5. Conclusions

(1) The performance of cascades varies substantially with aspect ratio

Cascade 5 gives higher deflection near stall and stalls earlier than cascade 2. The stall of cascade 5 is abrupt and is associated with a steep increase in total pressure loss and deviation and a sudden reduction in axial ratio. The stall of cascade 2 is gradual. The low aspect ratio produces greater contraction on the centreline, especially near stall.

(2) The enormous fluid contraction accounts for the deterioration in static pressure rise in both cases prior to stall.

(3) The nature of the end-wall stall changes with aspect ratio

The longer passage of the lower aspect ratio cascade gives the flow more time to rotate and the separation area is carried more along the blade than along the wall. In the other case, the separation areas on the end-wall and the blade are approximately equal.

(4) The cascade results are generally consistent with compressor results.

Acknowledgements

The author is indebted to Professor J. H. Horlock, Engineering Department, Cambridge University, and Professor J. F. Norbury, Department of Mechanical Engineering, Liverpool University, under whose supervision the work was carried out.

He would like to record his appreciation of the assistance given by the staff of the pattern workshop of the Department of Mechanical Engineering, Liverpool University, in the preparation of the equipment.

The British Ministry of Aviation sponsored the project and the Government of the United Arab Republic (Egypt) supported the author financially.

References

<u>No.</u>	<u>Author(s)</u>	<u>Title, etc.</u>
1	W. D. Armstrong	The Non-Uniform flow of Air through Cascades. Ph.D. Thesis, Cambridge University, (1954).
2	A. D. S. Carter	NGTE Memorandum M3, (1946).
3	A. D. S. Carter	The Low Speed Performance of Related Aerofoils in Cascade. ARC C.P.No.29, (1949).
4	J. R. Erwin and J. C. Emery	The Effect of Tunnel Configuration and Testing Technique on Cascade Performance. NACA T.N. No.2028, (1950).
5	G. J. S. Fahmi	The Effect of Blade Aspect Ratio on the Performance of Axial-Flow Compressors. Ph.D. Thesis, Liverpool University, (1967).
6	A. R. Felix and J. C. Emery	A Comparison of Typical National Gas Turbine Establishment and NACA Axial-Flow Compressor Blade Sections in Cascade at Low Speed. NACA T.N. No.3937, (1957).
7	J. P. Gostelow	The Accurate Prediction of Cascade Performance. Ph.D. Thesis, Liverpool University, (1965).
8	J. H. Horlock	Aerodynamics of Axial-Flow Turbomachines. Ph.D. Thesis, Cambridge University, (1955).
9	J. H. Horlock, P. M. E. Percival, J. F. Louis and B. Lakshiminarayana	Wall Stall in Compressor Cascades. Journal of Basic Engineering. Trans. ASME, Vol.81, Series D, (1959).

<u>No.</u>	<u>Author(s)</u>	<u>Title, etc.</u>
10	J. H. Horlock, R. Shaw, D. Pollard and A. K. Lewkowicz	Reynolds Number Effects in Cascades and Axial-Flow Compressors. Journal of Engineering for Power. Trans. ASME, Vol.86, Series A, pp.236-242. (1964).
11	A. R. Howell	The Present Basis of Axial Flow Compressor Design. ARC R. & M. 2095 (1942).
12	-	Preliminary Report on the Influence of Aspect Ratio on the Performance of Axial-Flow Compressors. Rep. No. 1062-1, (1963). Northern Research and Engineering Corporation.
13	D. Pollard	Low Speed Performance of Two-Dimensional Cascades of Aerofoils. Ph. D. Thesis, Liverpool University (1964).
14	D. Pollard and J. P. Gostelow	Some Experiments at Low Speed on Compressor Cascades. Journal of Engineering for Power. Trans. ASME, Vol. 89, Series A, No. 3, pp. 427-436. (1967).
15	H. G. Rhoden	Effects of Reynolds Number on the Flow of Air through a Cascade of Compressor Blades. ARC R. & M. 2919. (1952).
16	C. Rouffignac	Behaviour of Compressor Cascades of different Curvature and Aspect Ratios. ONERA TN 39, 1957.
17	M. R. A. Shaalan	The Stalling Performance of Compressor Cascades of Different Aspect Ratios. Ph.D.Thesis, Liverpool University, (1967).
18	A. Smith	Development in Techniques of Measuring Representative Mid-span Losses of Turbine Blades in Cascade. A.R.C. 29 244 - P.A.1233 (1967).

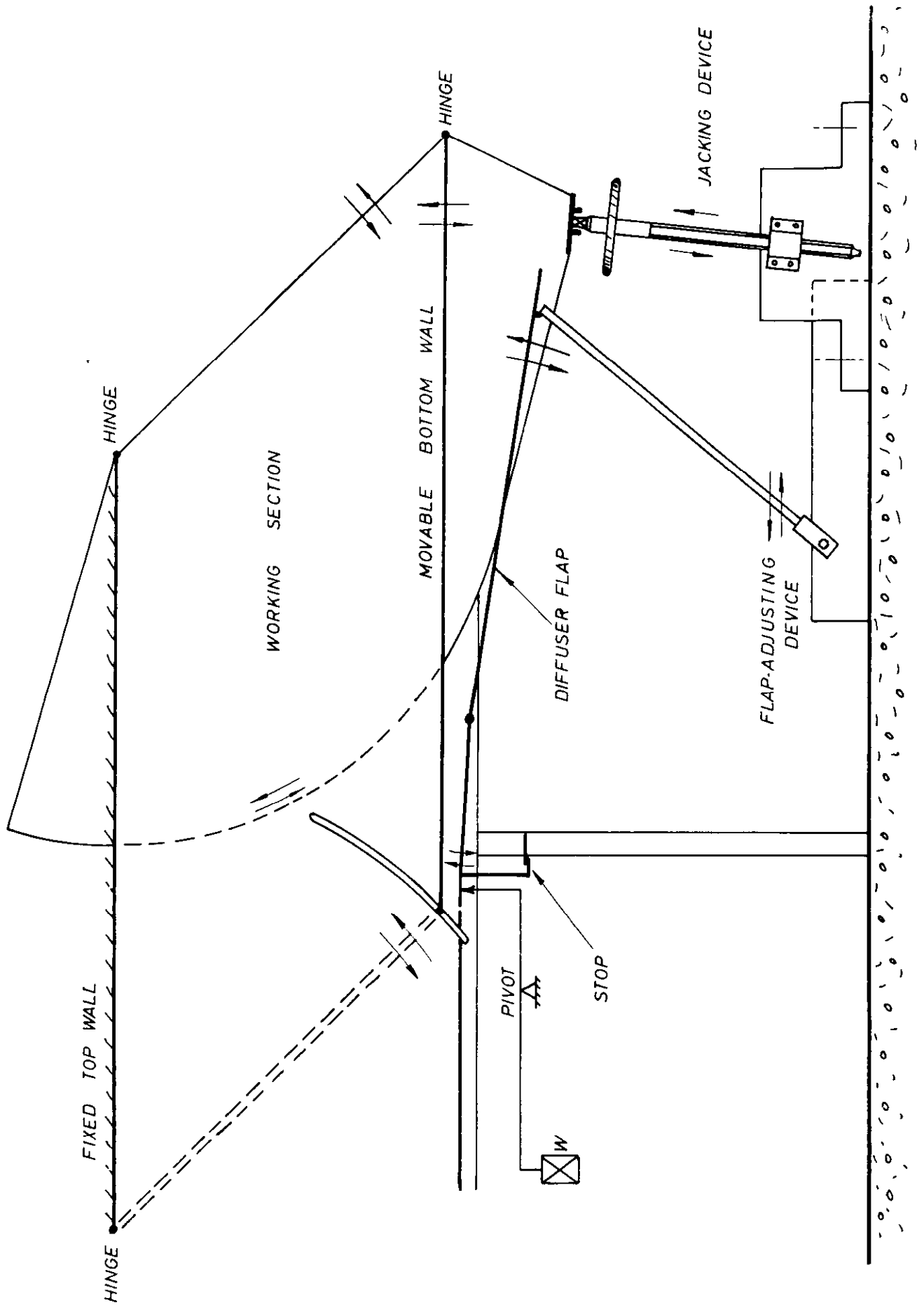


FIG 1 MECHANISM FOR INCIDENCE VARYING

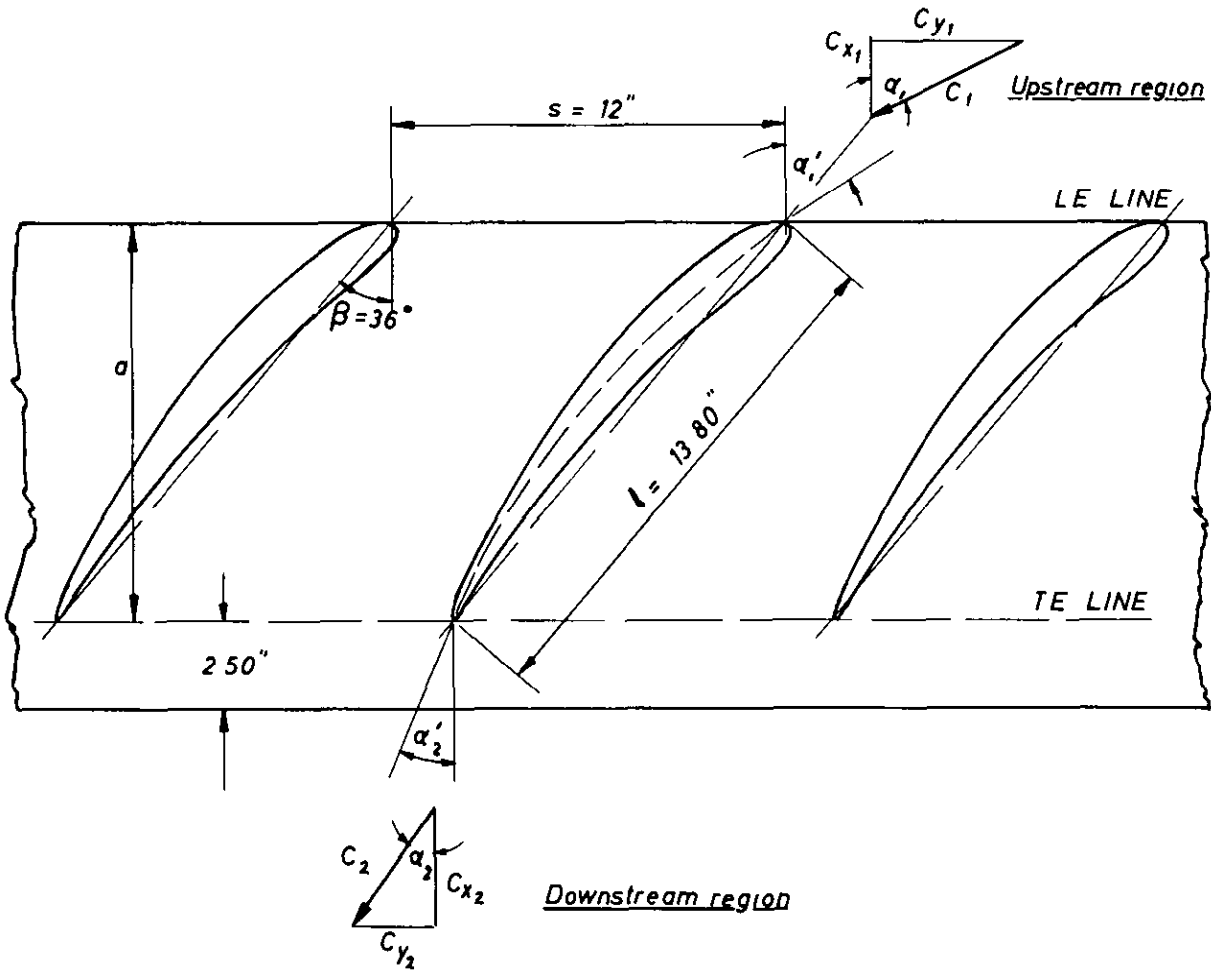
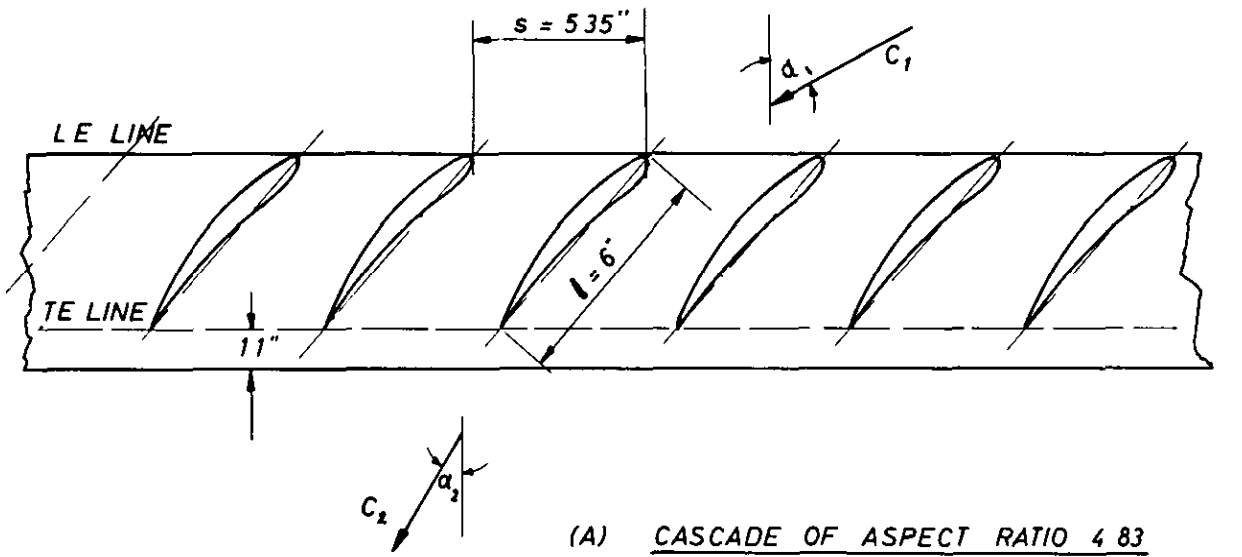


FIG 2 GEOMETRY OF THE EXPERIMENTAL CASCADES

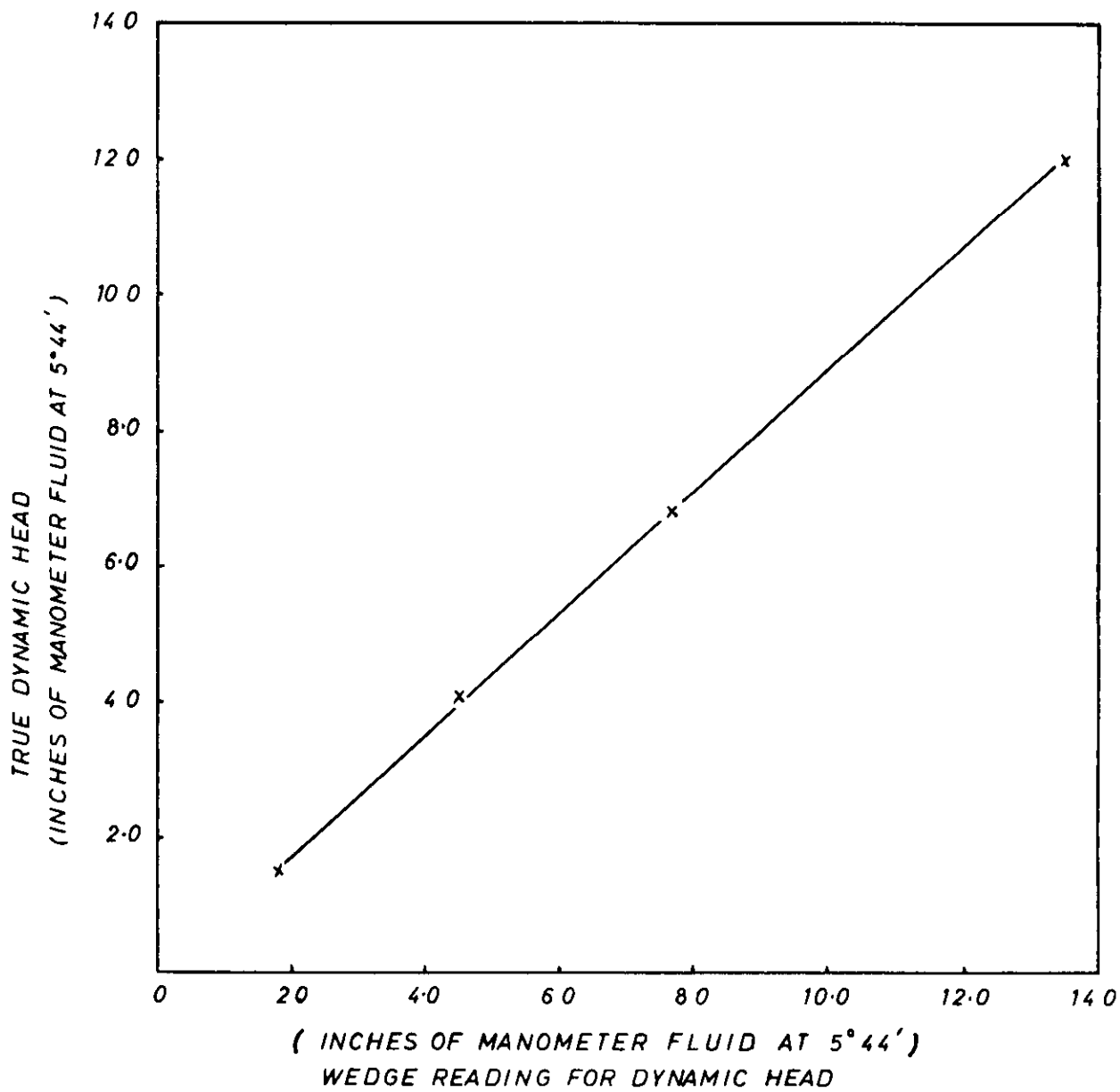


FIG. 3 WEDGE INSTRUMENT CALIBRATION CURVE (TYPICAL RESULT)

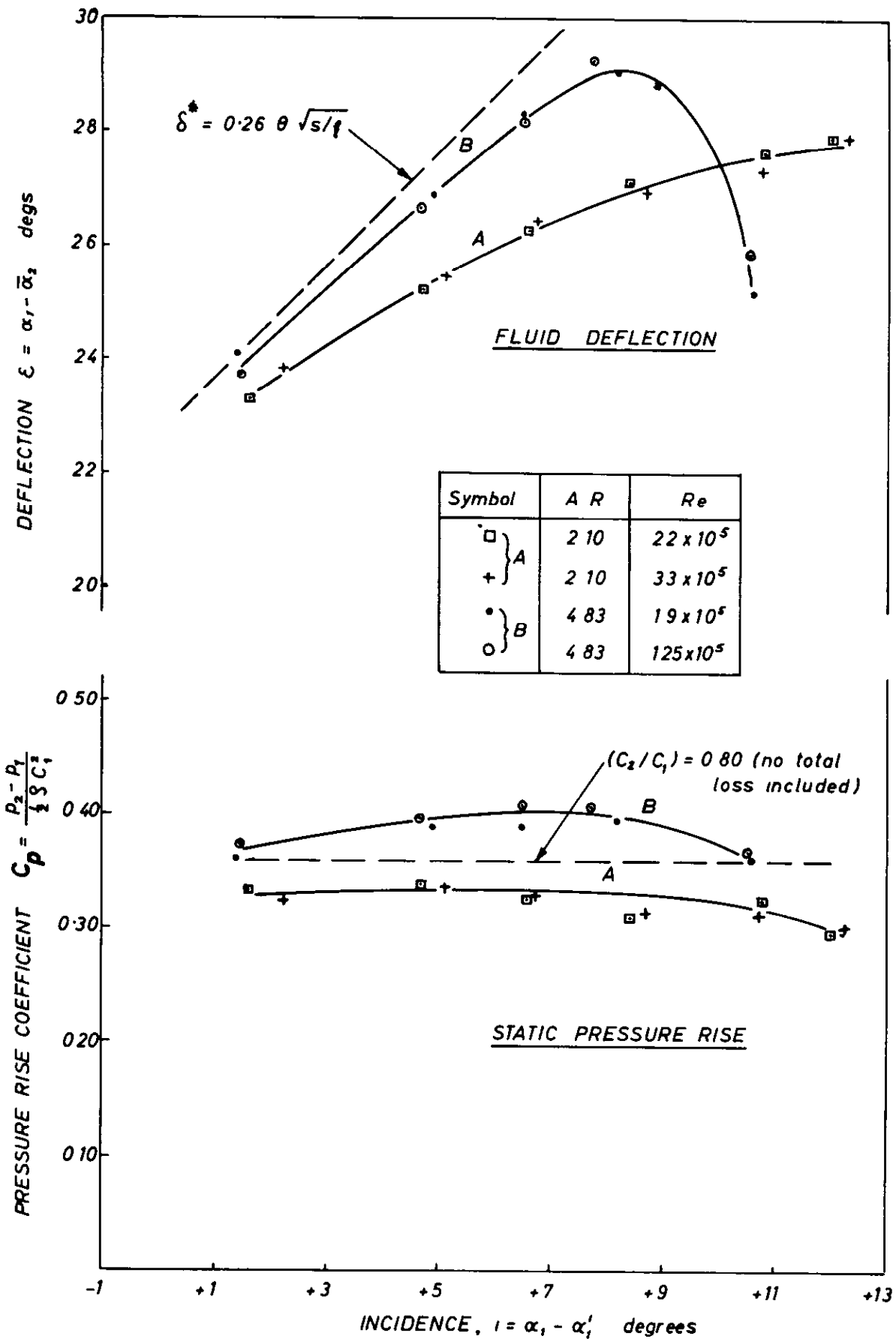


FIG 4 EXPERIMENT - PERFORMANCE OF TWO CASCADES OF DIFFERENT ASPECT RATIOS PRESSURE RISE AND DEFLECTION

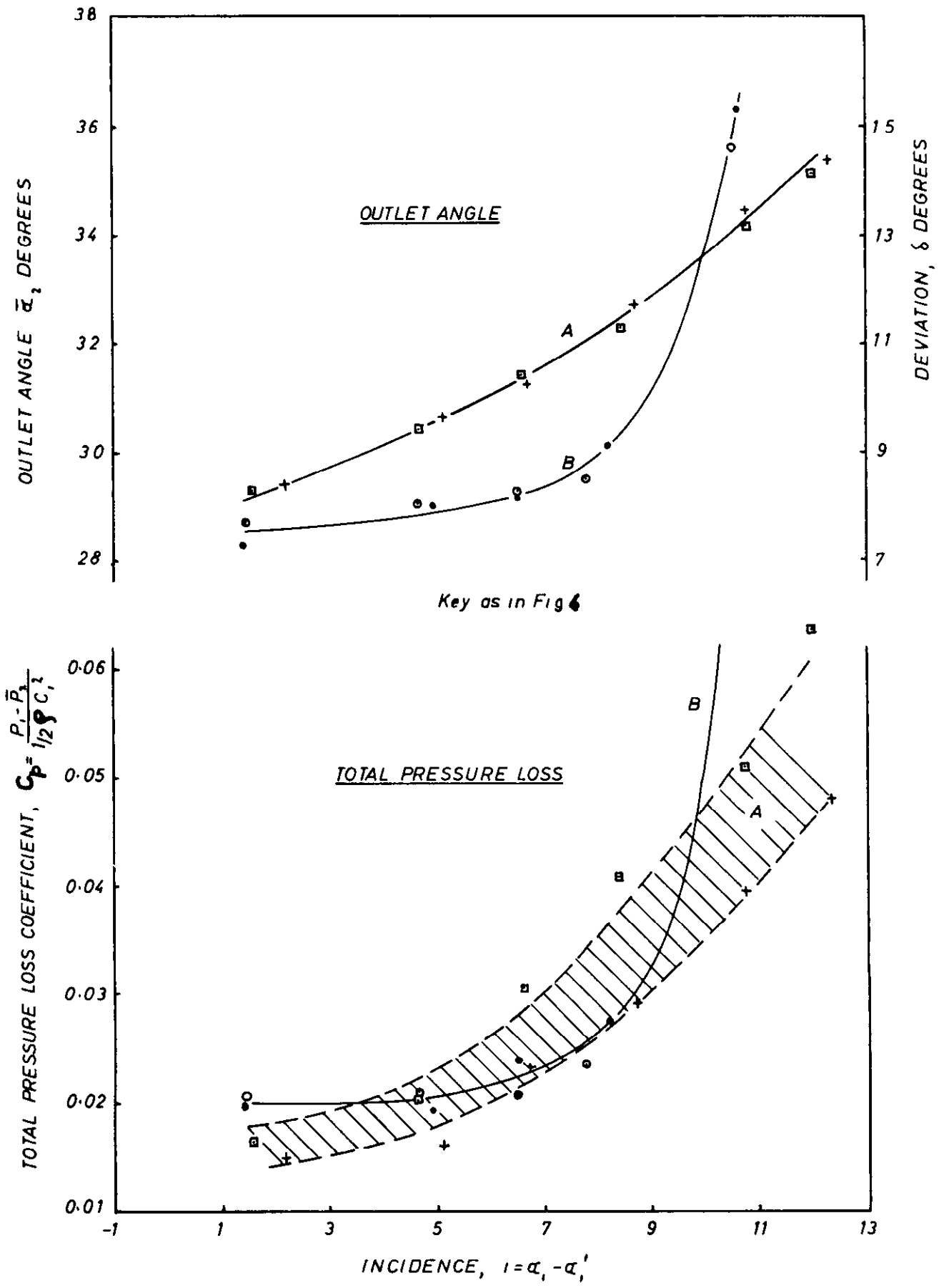


FIG.5 EXPERIMENT-PERFORMANCE OF TWO CASCADES OF DIFFERENT ASPECT RATIOS : MID-SECTION OUTLET ANGLE AND TOTAL PRESSURE LOSS

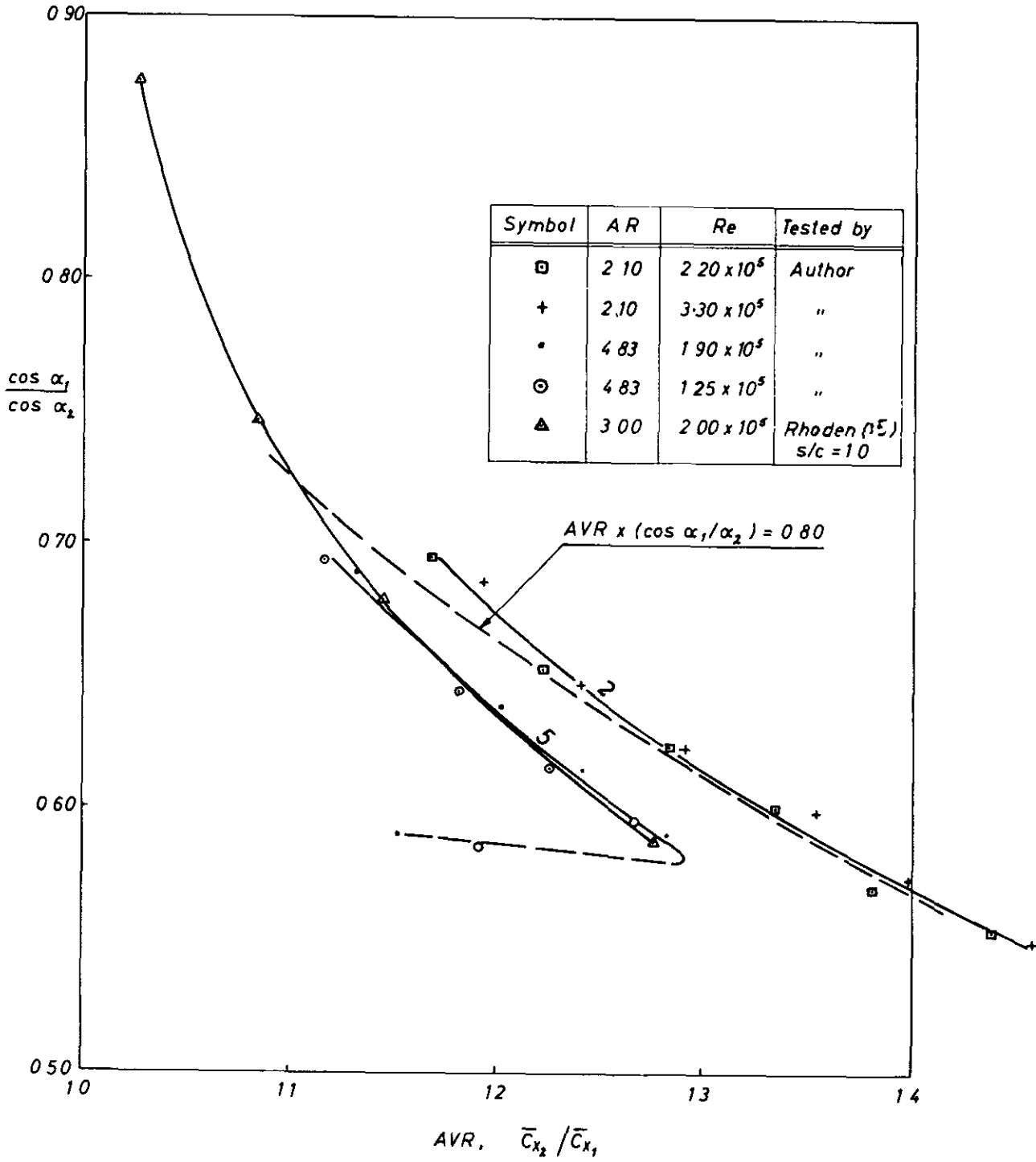


FIG. 6 EXPERIMENT - AXIAL VELOCITY RATIO AS A FUNCTION OF $\frac{\cos \alpha_1}{\cos \alpha_2}$

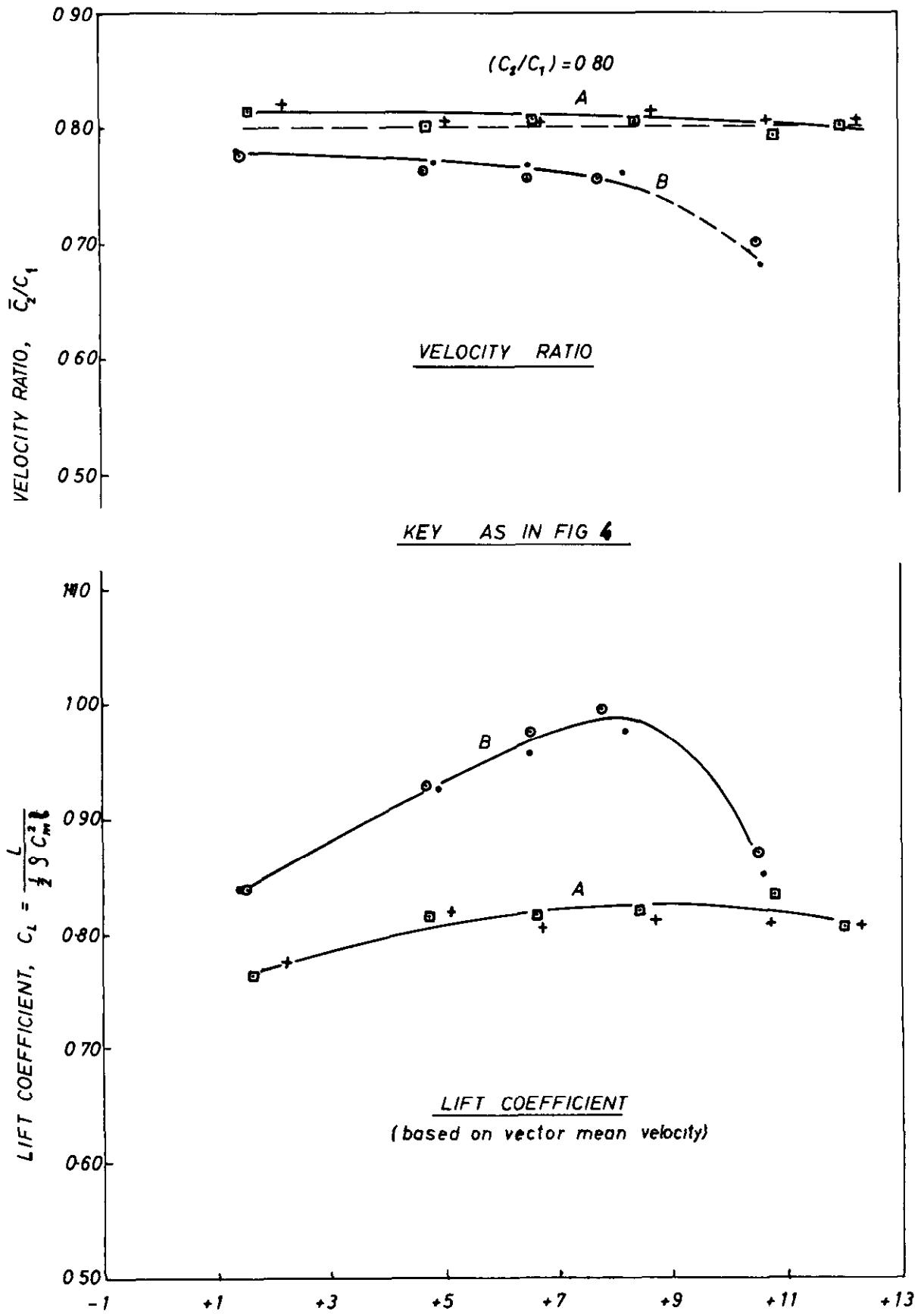
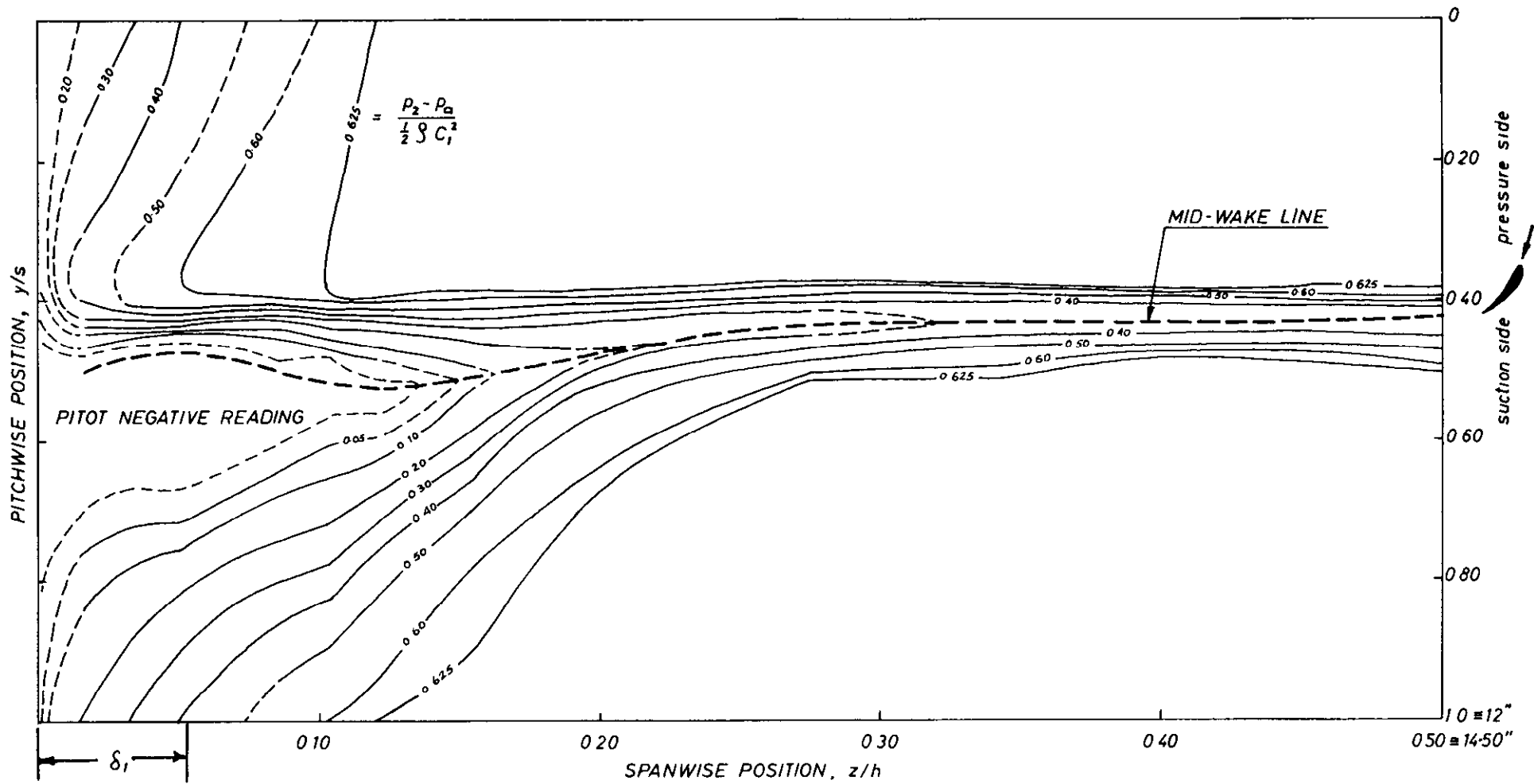


FIG. 7 EXPERIMENT-PERFORMANCE OF TWO CASCADES OF DIFFERENT ASPECT RATIOS: VELOCITY RATIO AND LIFT COEFFICIENT

FIG. 8 TOTAL PRESSURE CONTOURS FOR $AR=2$ NEAR DESIGN
 ($\alpha = 1.50^\circ$ $Re = 2.2 \times 10^5$)



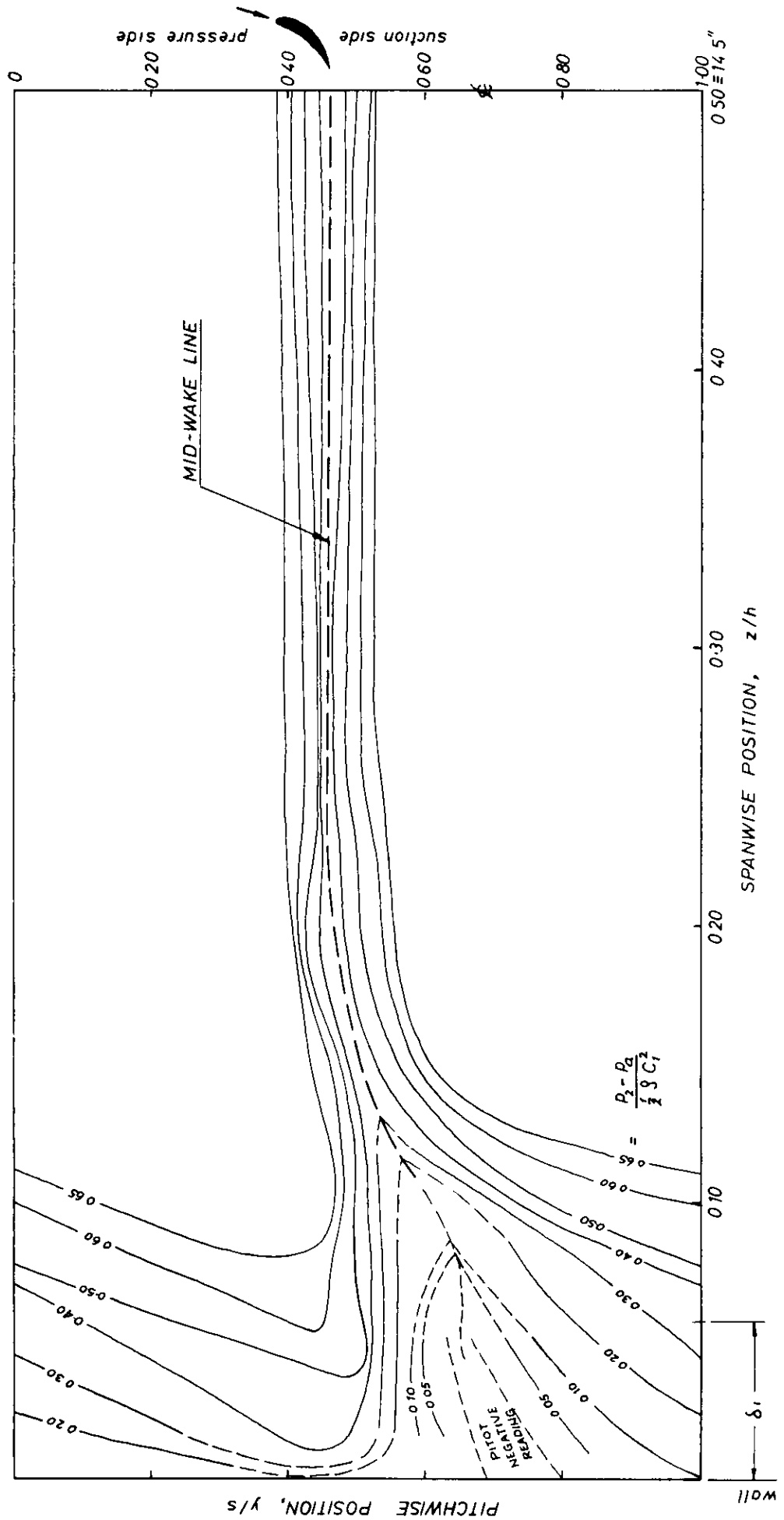


FIG. 9 TOTAL PRESSURE CONTOURS FOR AR=5 NEAR DESIGN
($\alpha = 1.70^\circ$ $Re = 1.80 \times 10^5$)

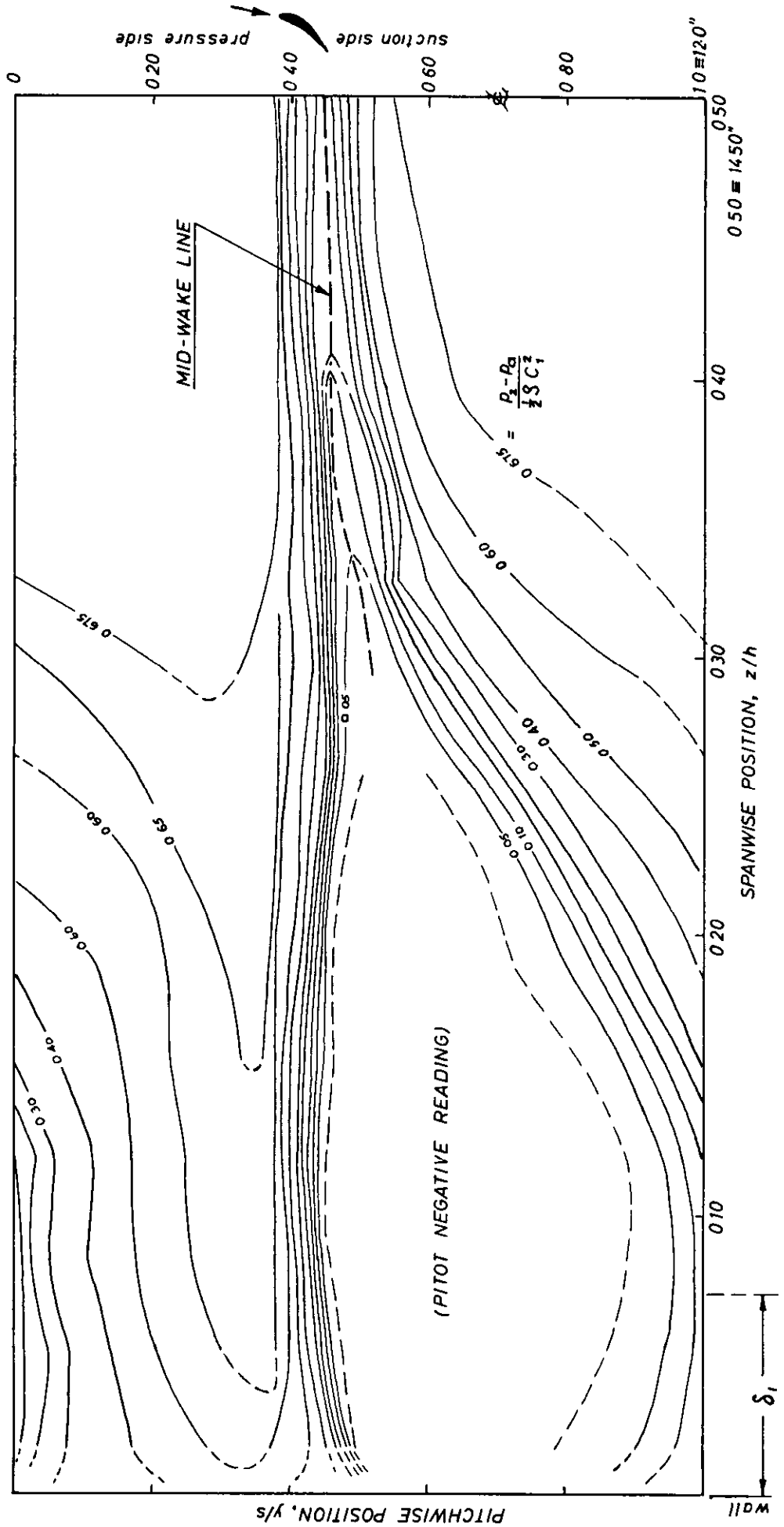


FIG.10 EXPERIMENT-TOTAL PRESSURE CONTOURS FOR AR=2 NEAR STALL
 ($\alpha = 8.40^\circ$ $Re = 2.20 \times 10^5$)

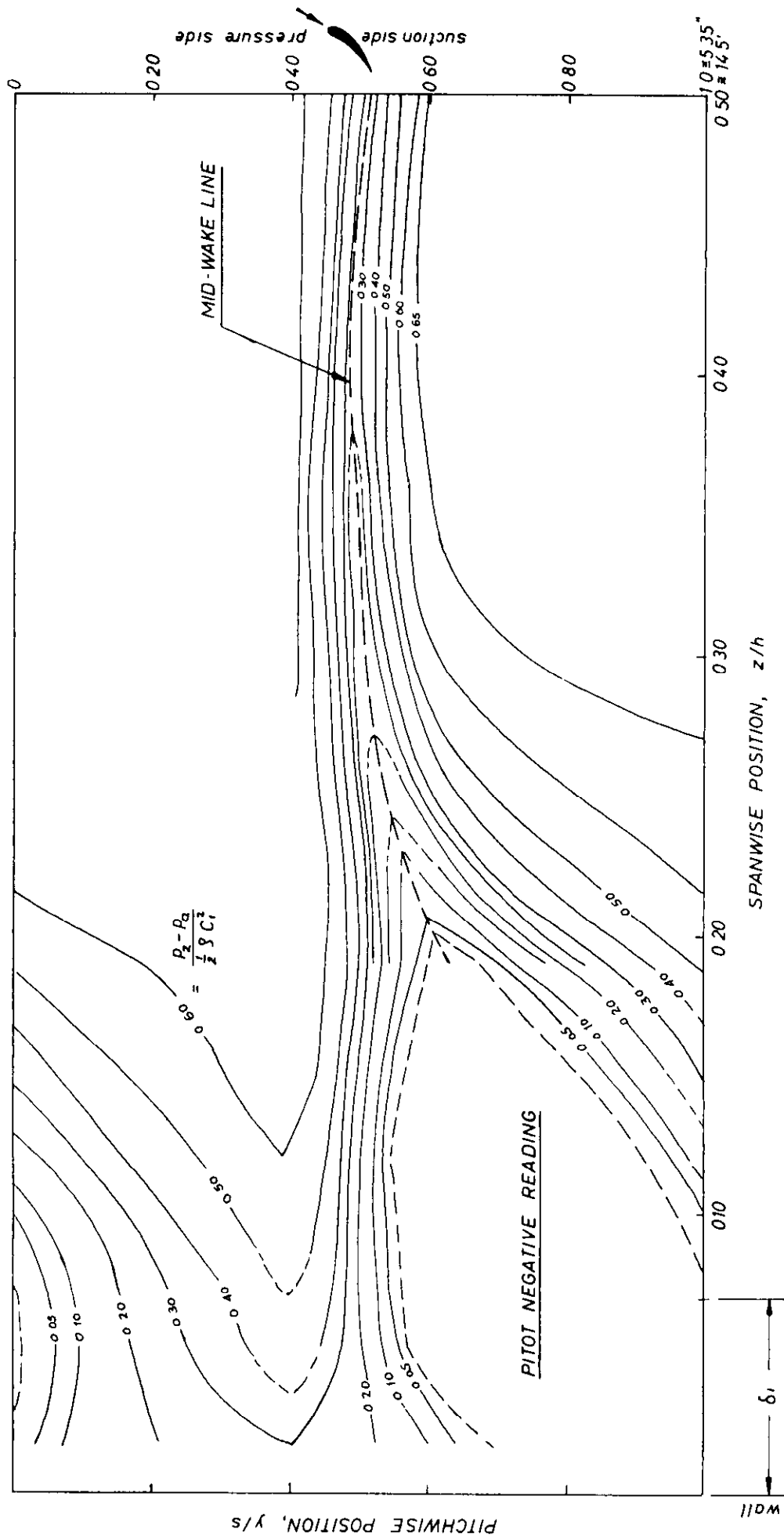


FIG.11 TOTAL PRESSURE CONTOURS FOR AR=5 NEAR STALL
($\alpha = 8.20^\circ$ $Re = 1.80 \times 10^5$)

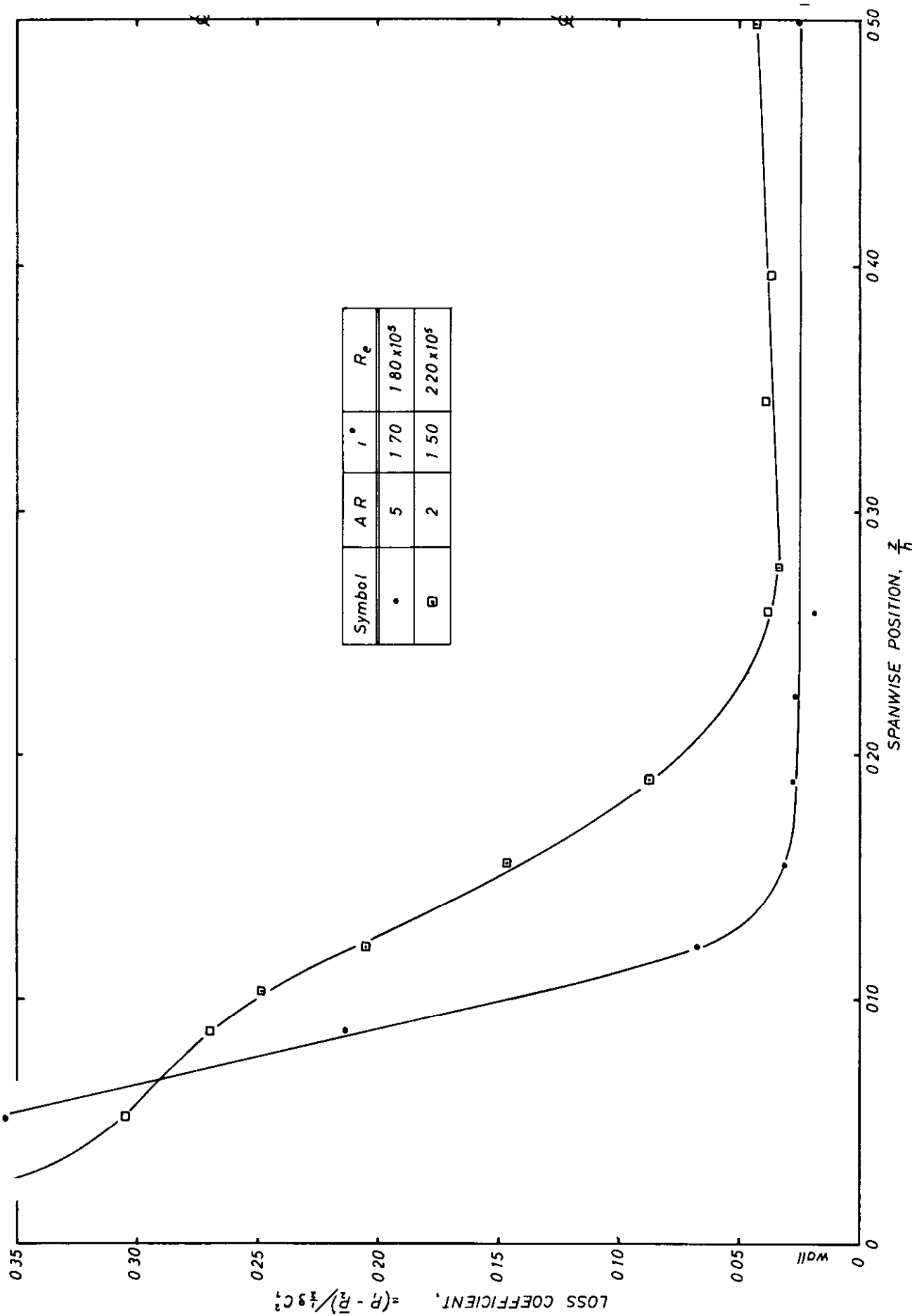


FIG.12 EXPERIMENT INTEGRATED TOTAL PRESSURE LOSS (near-design conditions)

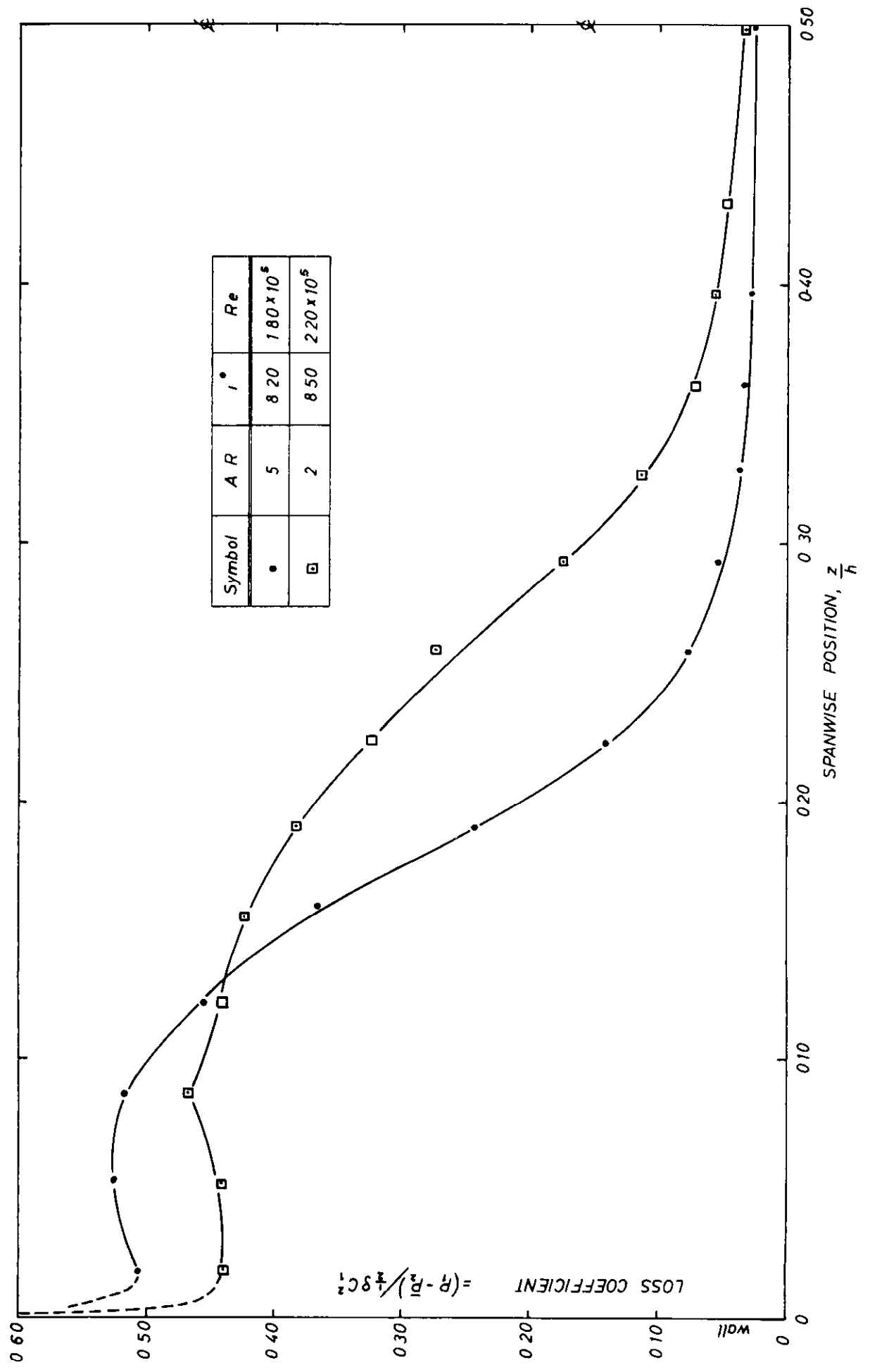


FIG.13 EXPERIMENT- INTEGRATED TOTAL PRESSURE LOSS (near-stall conditions)

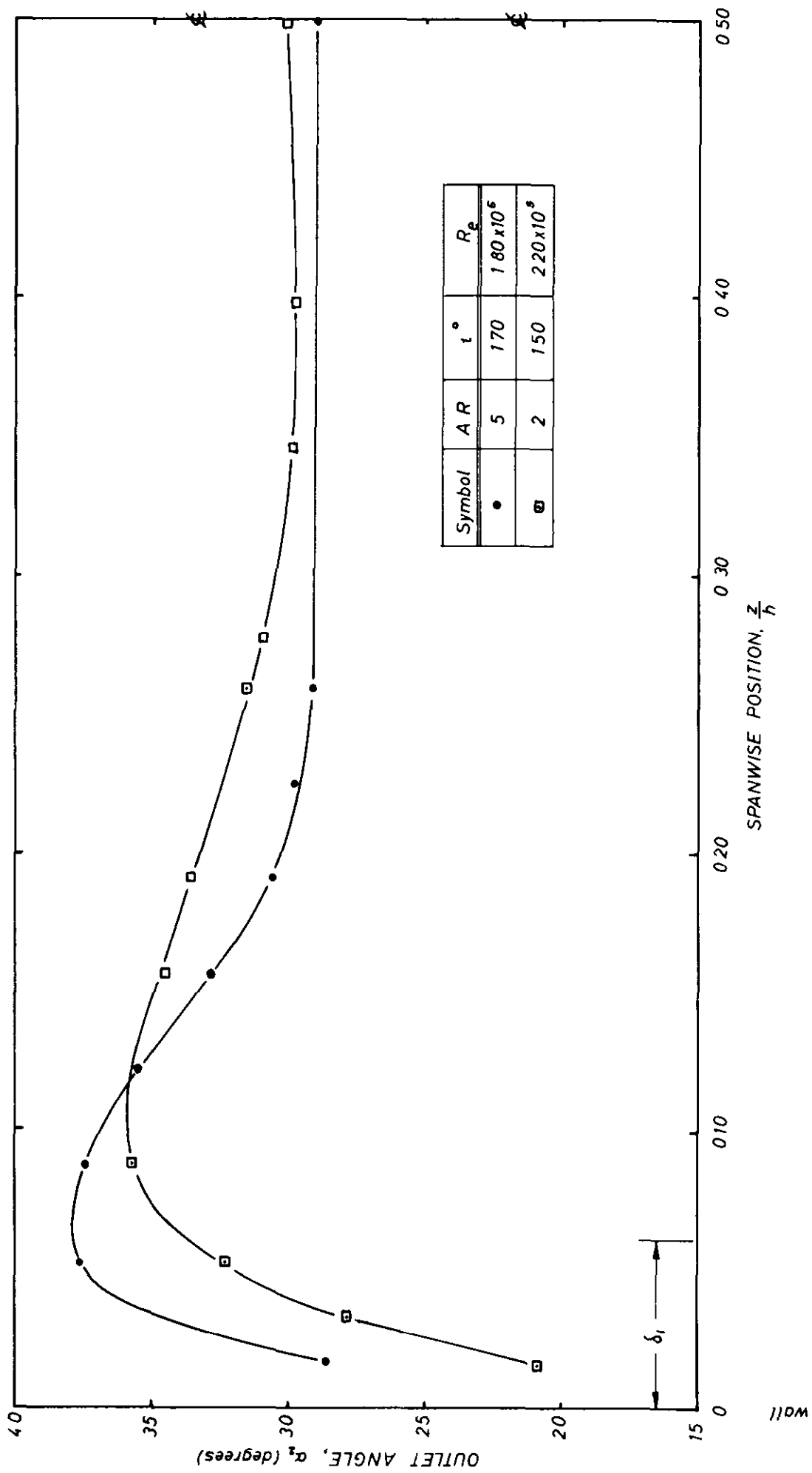


FIG.14 EXPERIMENT-OUTFLOW ANGLE AT MID-PITCH POSITION (near design)

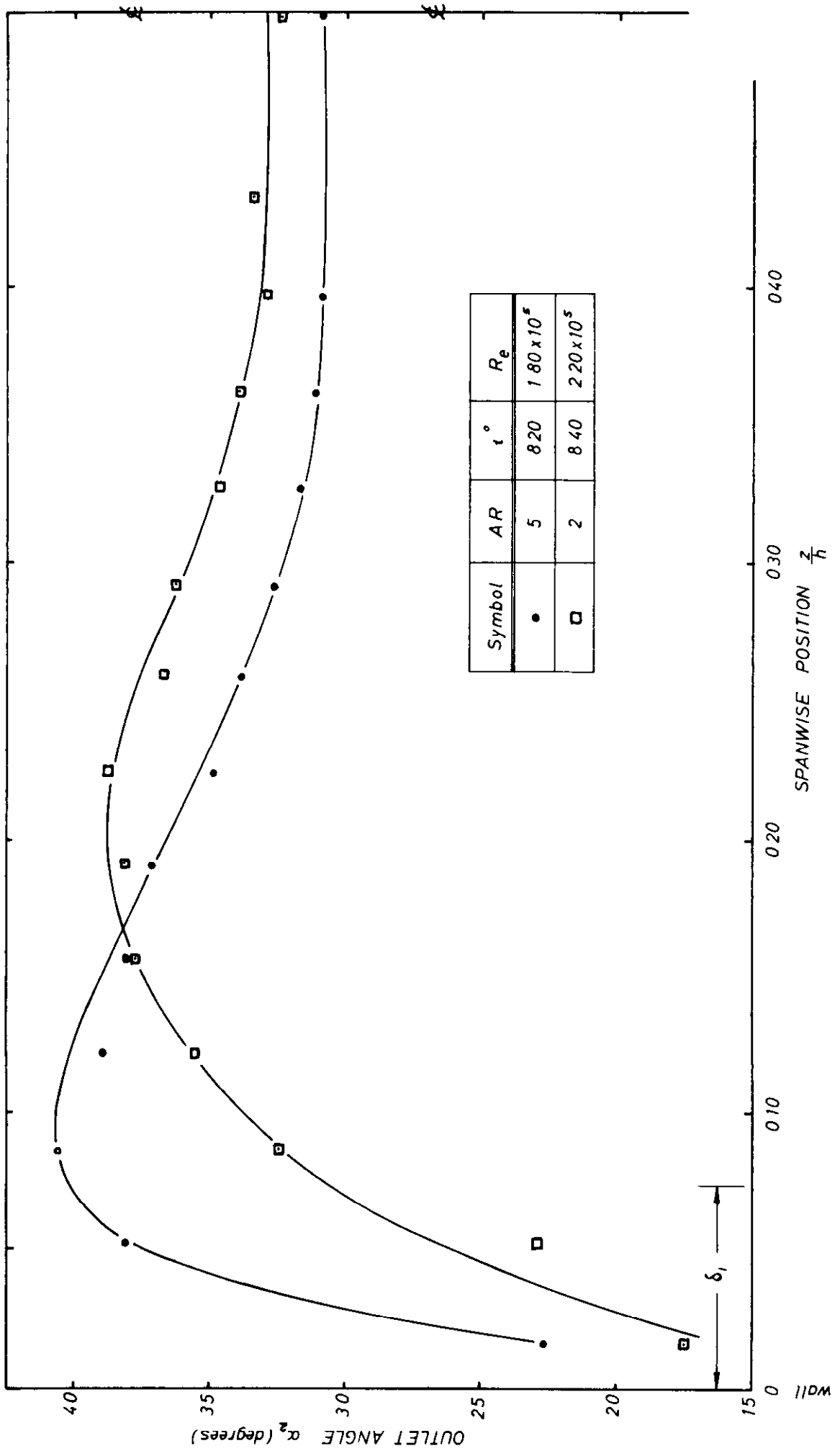


FIG 15 EXPERIMENT - OUTFLOW ANGLE AT MID-PITCH POSITION (near-stall conditions)

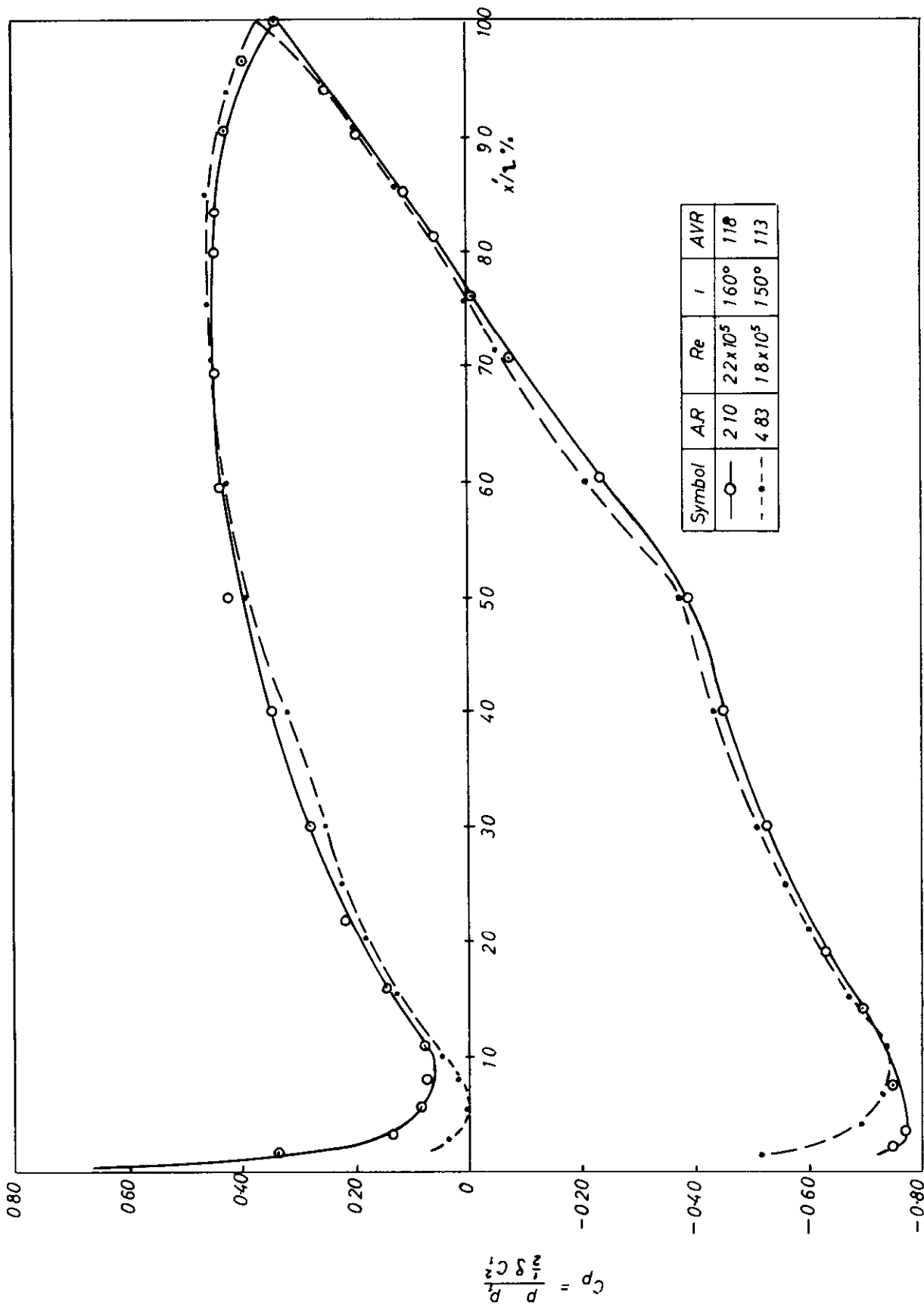


FIG 16 EXPERIMENT-COMPARISON BETWEEN PRESSURE DISTRIBUTION FOR TWO ASPECT RATIOS (mid section near design)

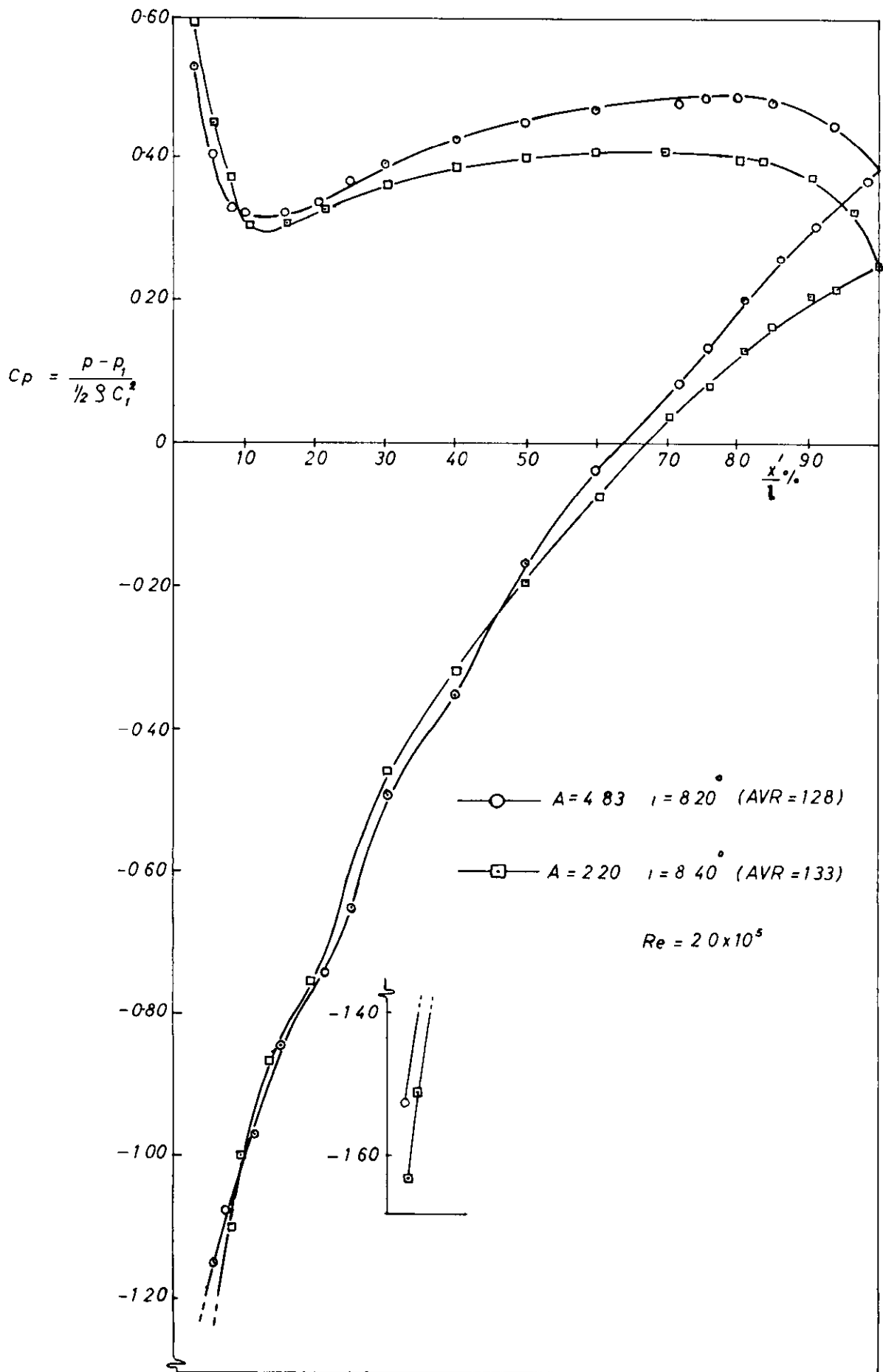


FIG 17 EXPERIMENT - COMPARISON OF PRESSURE DISTRIBUTIONS AT NEAR-STALL CONDITIONS

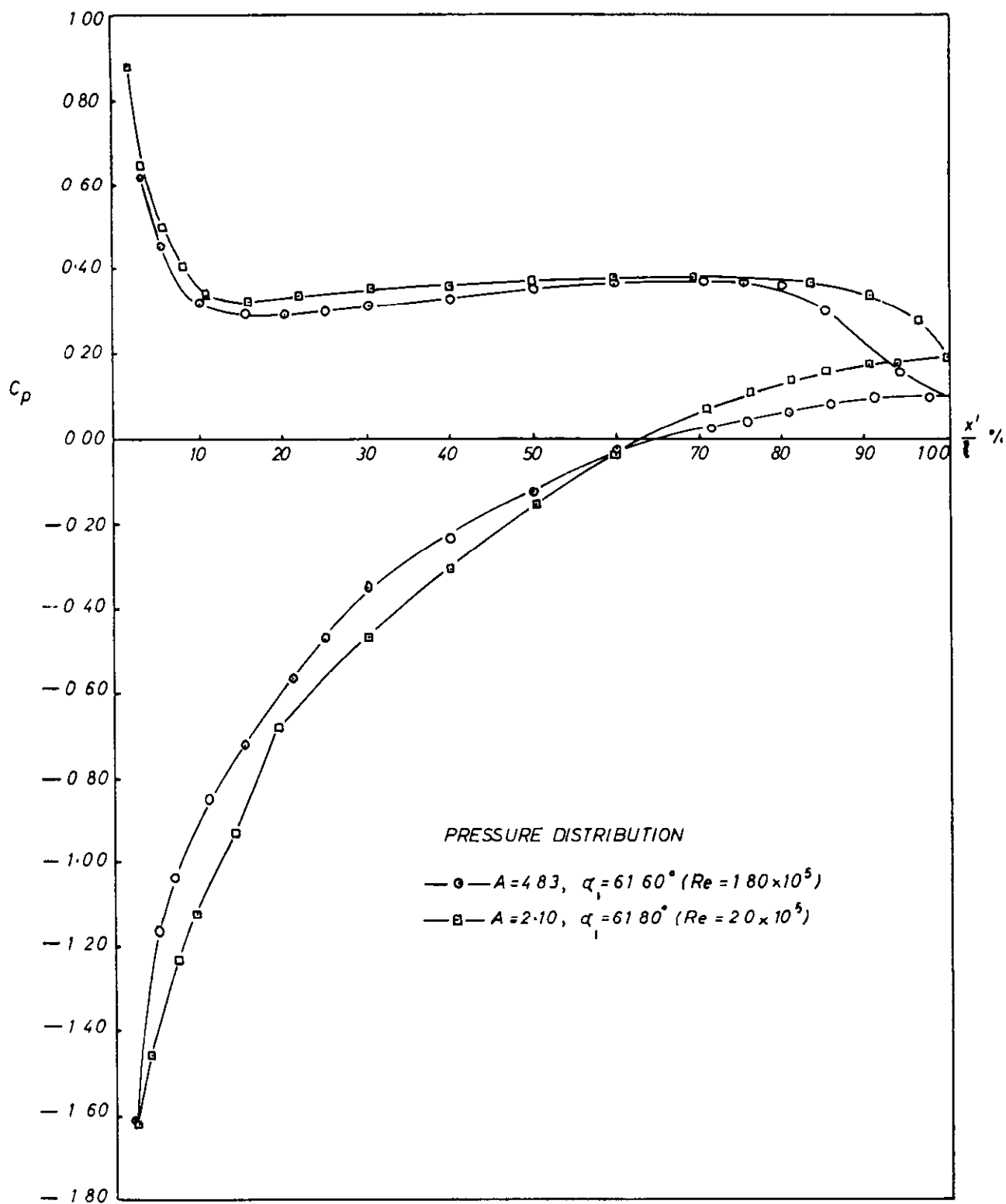


FIG. 18 EXPERIMENT-COMPARISON OF PRESSURE DISTRIBUTIONS
AT STALLED CONDITIONS

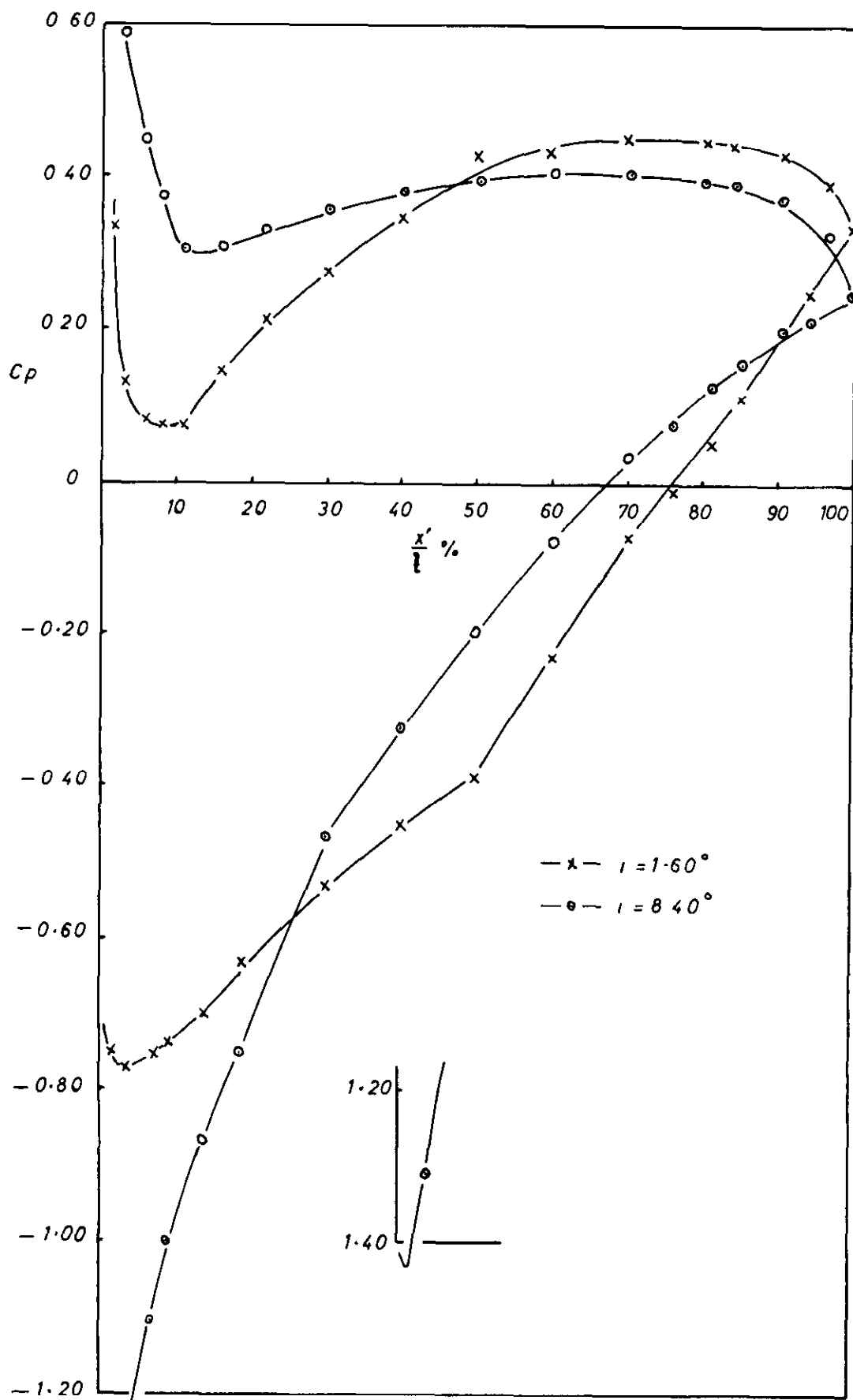


FIG.19 EXPERIMENT COMPARISON OF PRESSURE DISTRIBUTIONS AT LOW AND HIGH INCIDENCE (A.R.=2.10)

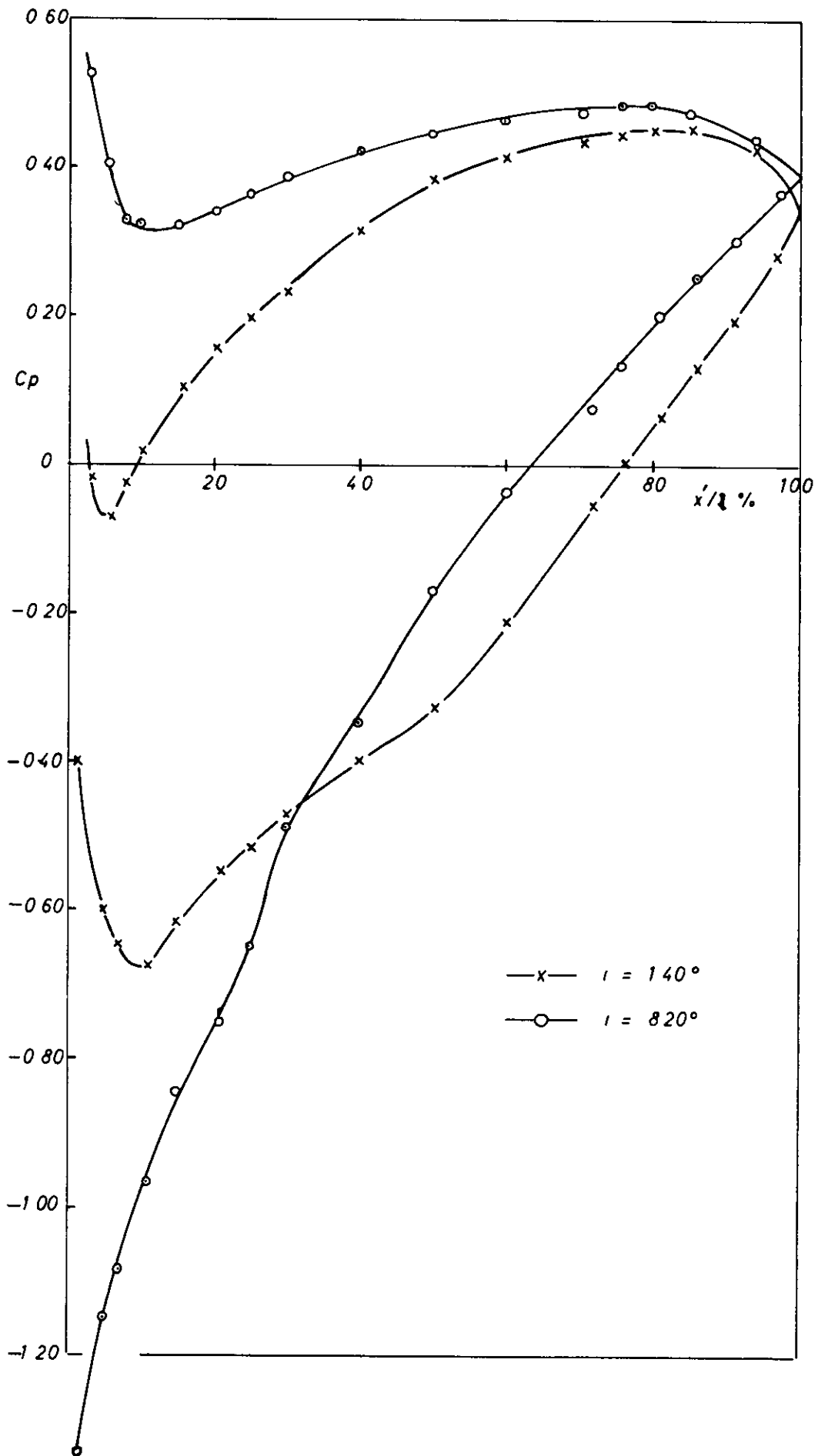


FIG. 20 EXPERIMENT-COMPARISON OF PRESSURE DISTRIBUTIONS AT LOW AND HIGH INCIDENCE (AR=4.83)

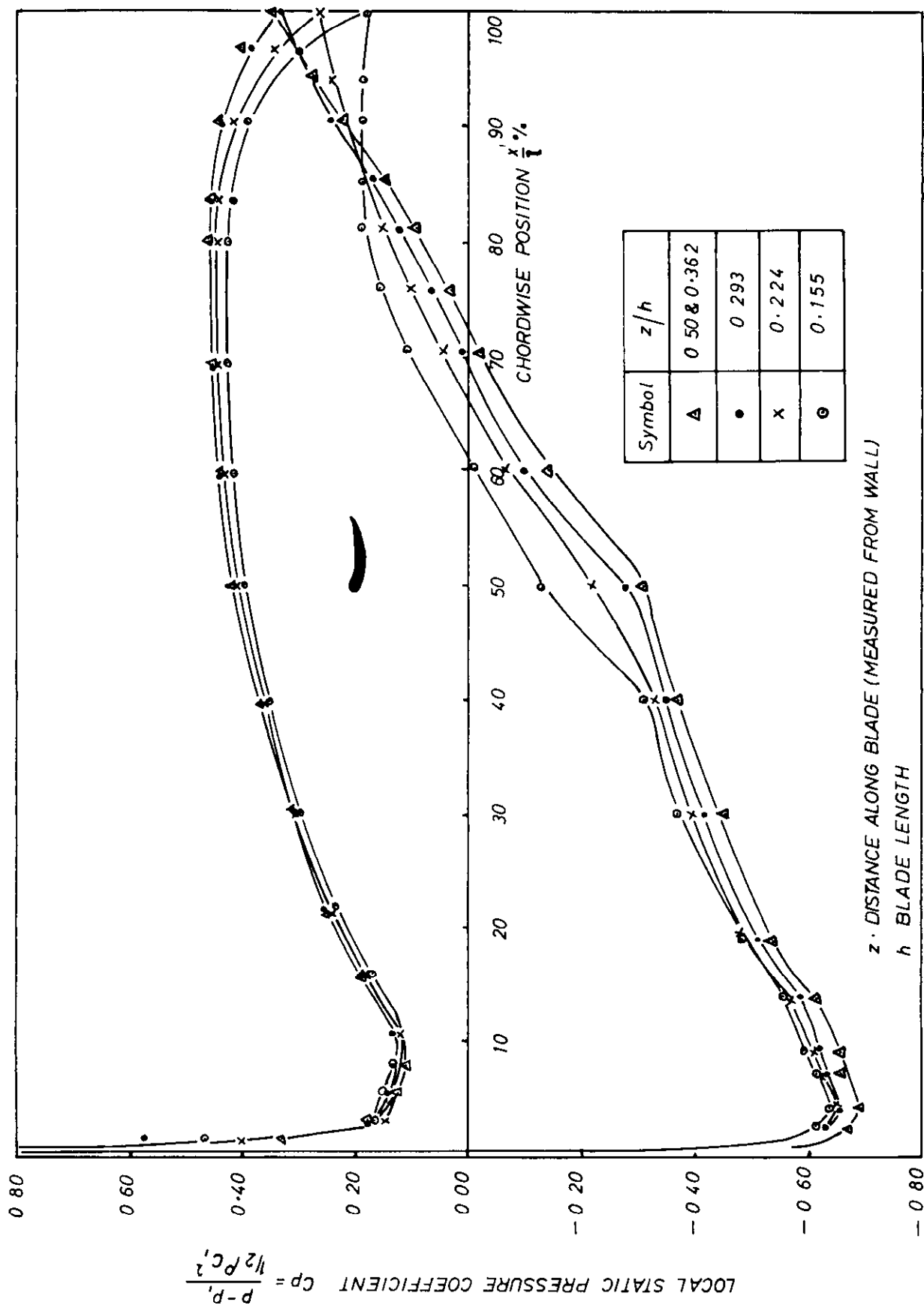


FIG 21 EXPERIMENT-PROFILE PRESSURE DISTRIBUTION AT DIFFERENT SPANWISE POSITIONS

(A $R. = 2$, NEAR DESIGN ($i = 170^\circ$), $Re = 2.20 \times 10^5$)

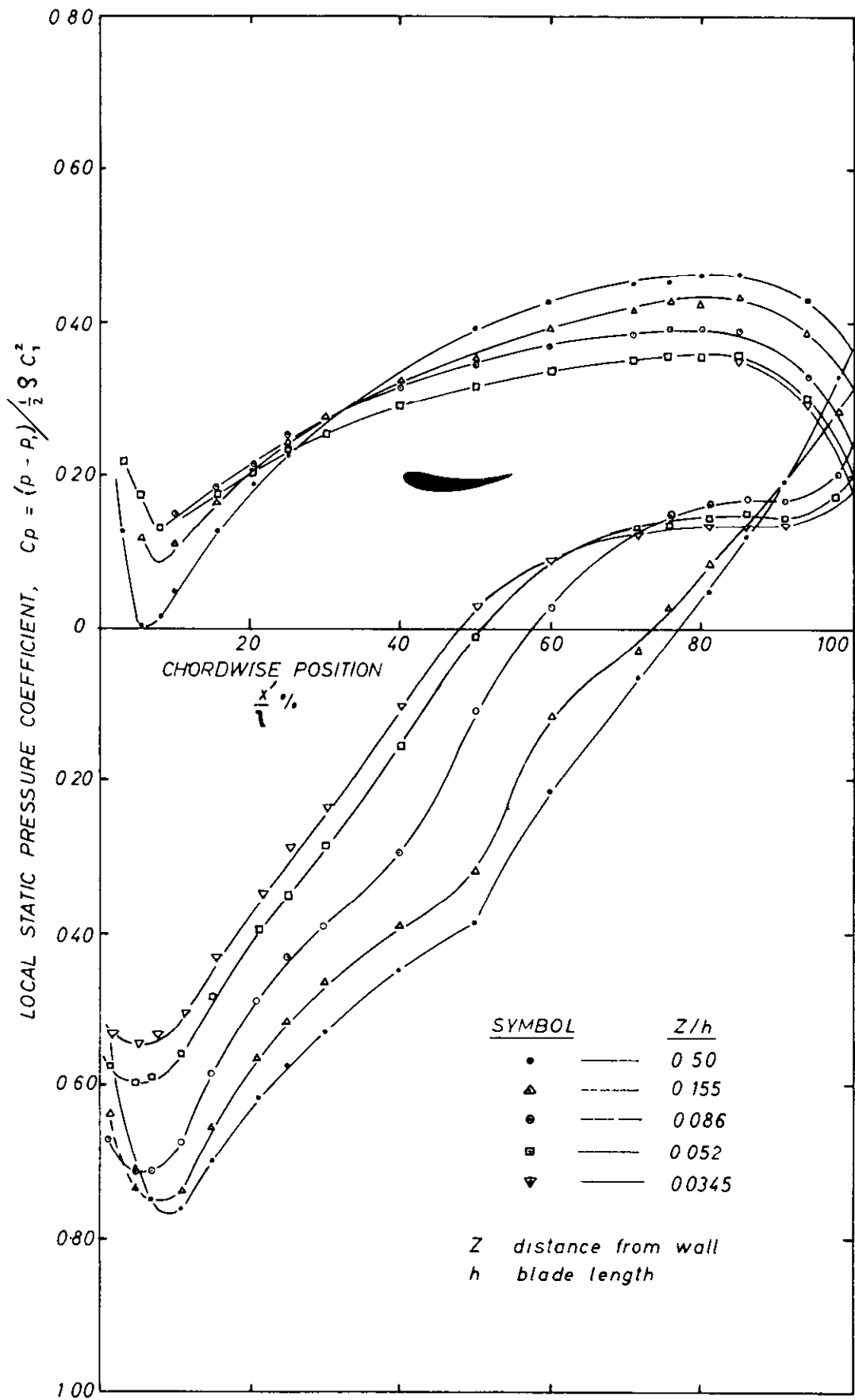


FIG 22 EXPERIMENT - PROFILE PRESSURE DISTRIBUTION AT DIFFERENT SPANWISE POSITIONS FOR $AR=5$ NEAR DESIGN ($\alpha=140^\circ$ $Re=180 \times 10^5$)

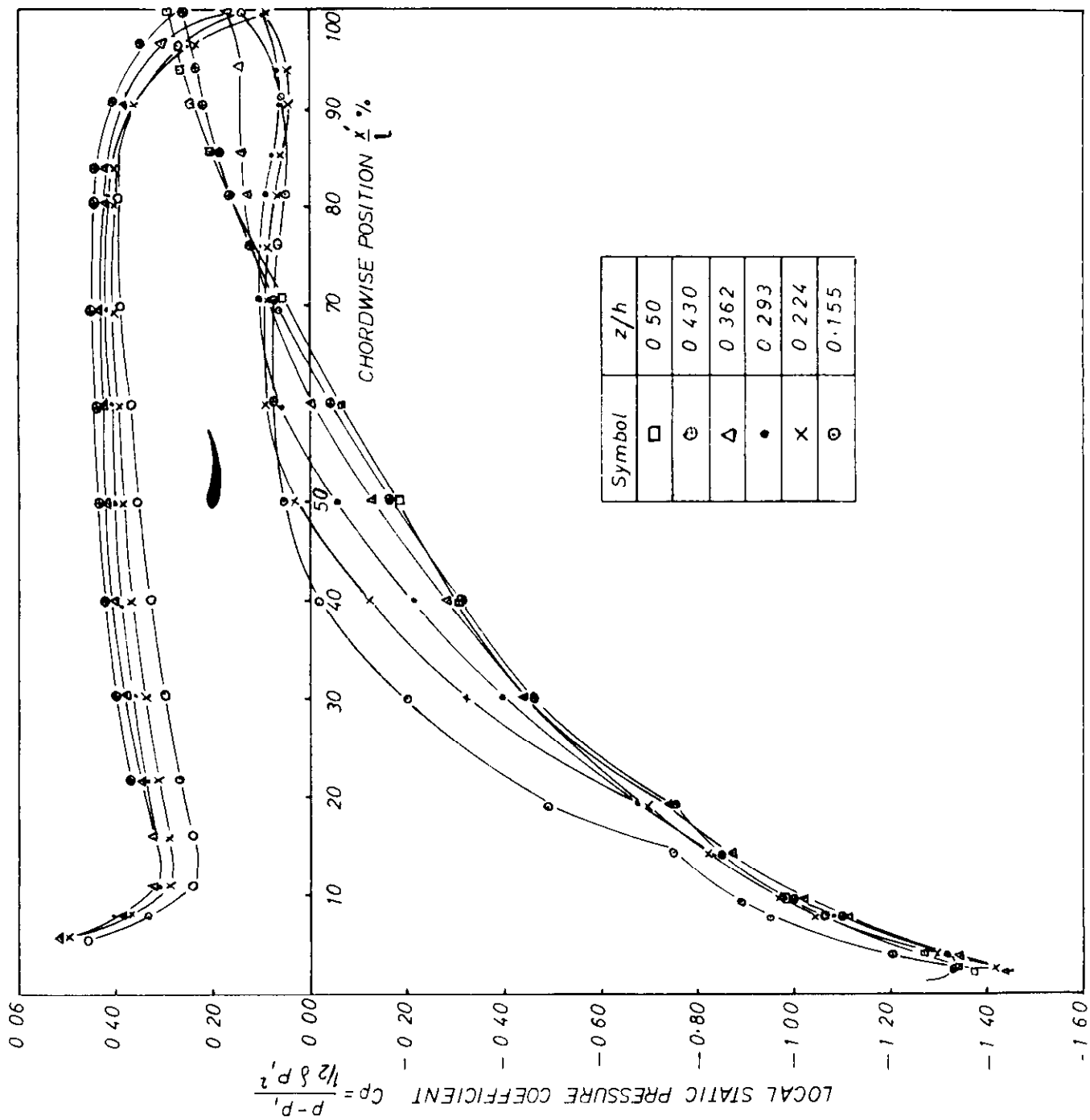


FIG 23 EXPERIMENT-PROFILE PRESSURE DISTRIBUTION AT DIFFERENT SPANWISE POSITIONS

($AR=2$, $NEAR\ STALL\ (\alpha=8.50)$, $Re = 2.20 \times 10^5$)

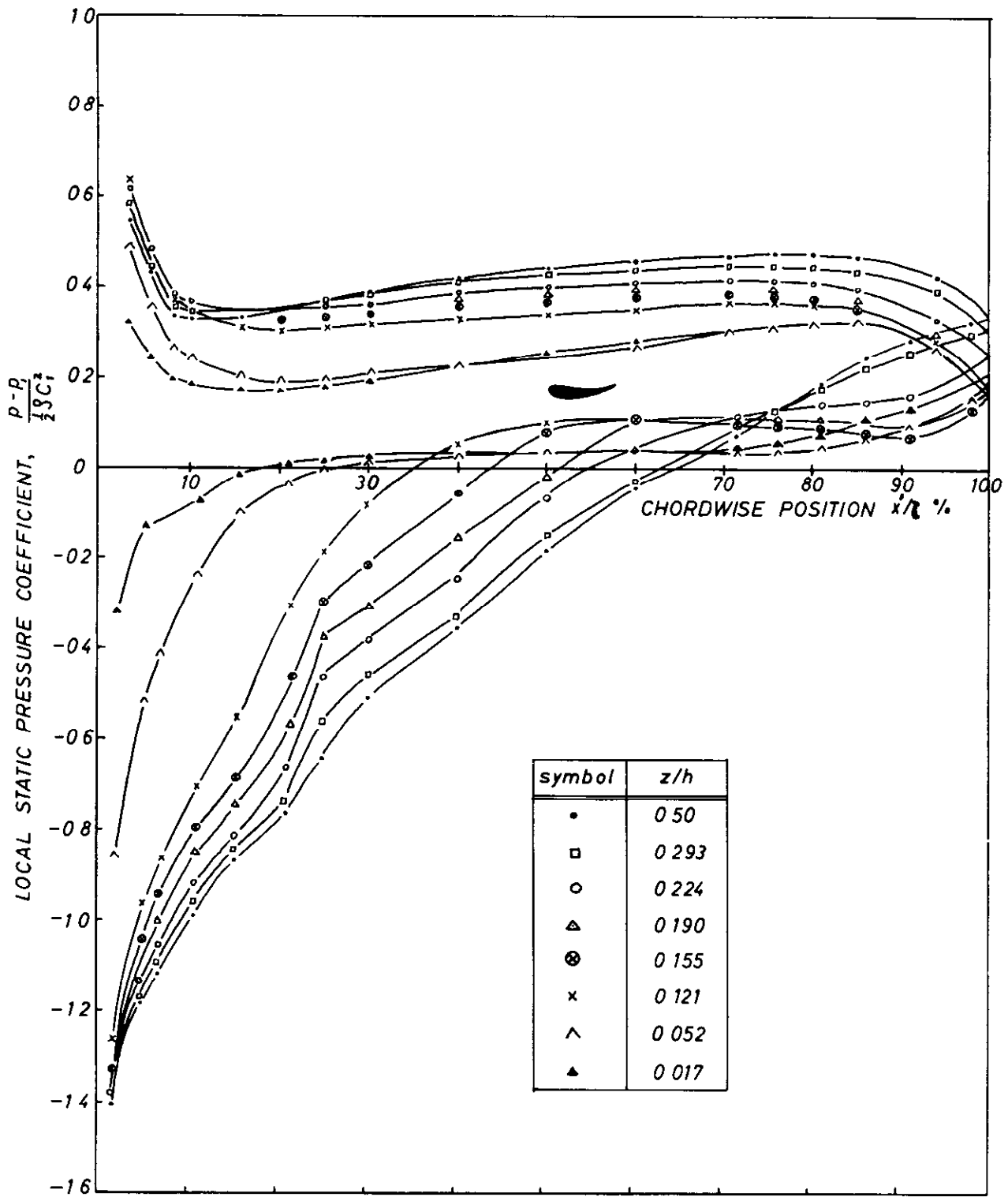


FIG 24 EXPERIMENT-PROFILE PRESSURE DISTRIBUTION AT DIFFERENT SPANWISE POSITIONS (AR = 5 NEAR STALL ($\alpha = 8.3^\circ$) $Re = 180 \times 10^5$)

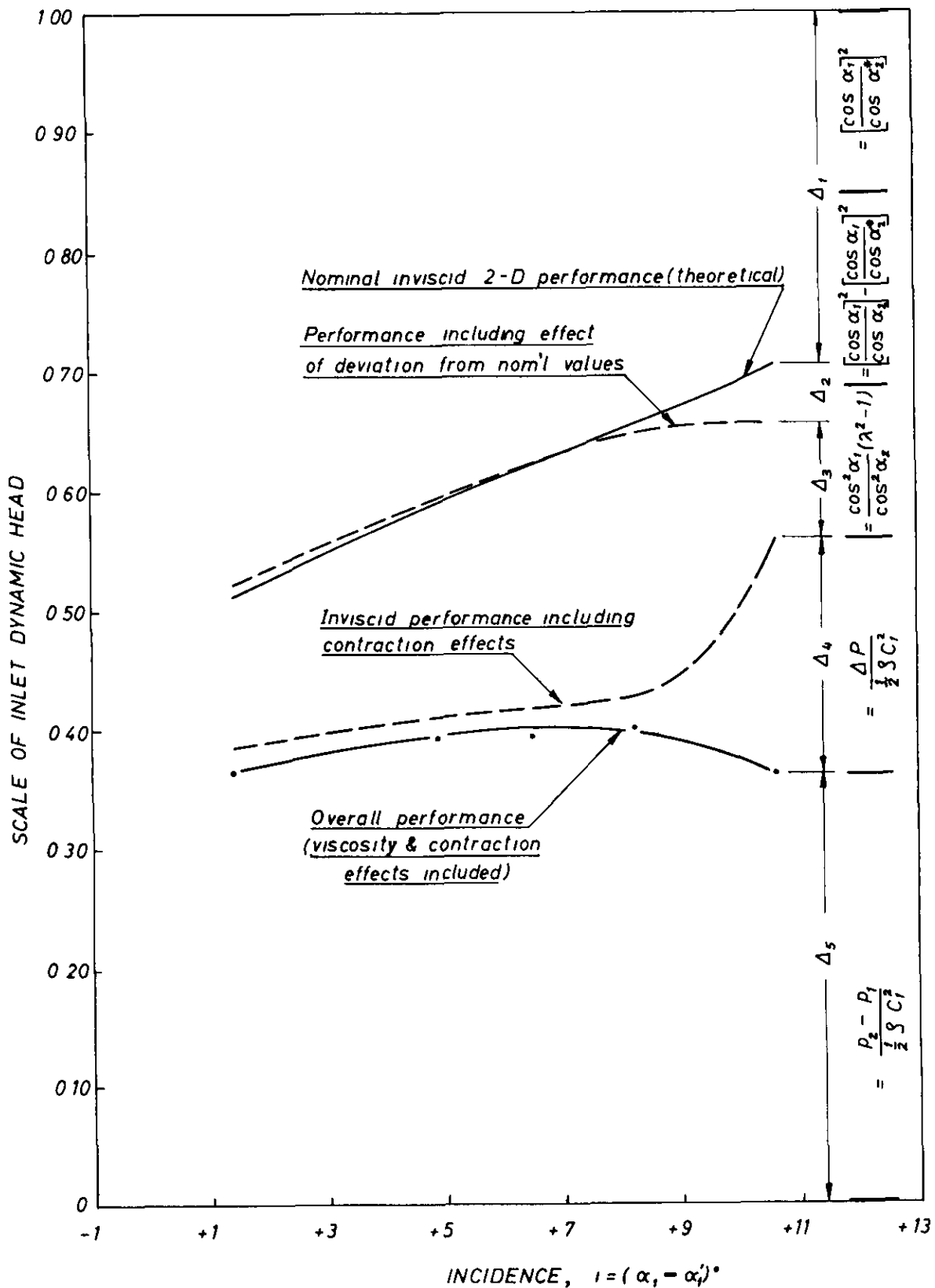


FIG. 25 FRACTIONAL CHANGES IN DYNAMIC HEAD IN COMPRESSOR CASCADES (AR = 4.83)



A.R.C. C.P. No.1103
28th March, 1968
M.R.A. Shaalan

A WIND-TUNNEL INVESTIGATION OF THE STALLING PERFORMANCE
OF TWO COMPRESSOR CASCADES OF DIFFERENT ASPECT RATIOS
AT LOW SPEED

Two compressor cascades of aspect ratio 2.10 and 4.83 were tested up to the stall point in a working section with solid side walls. A change in aspect ratio was obtained by changing the blade chord only. The blade section profile was the 10C4/30C50, staggered at 36 degrees with a space-chord ratio of 0.88, and there was no tip clearance. Reynolds number similarity was maintained but its value was kept above a "critical" value.

The/

A.R.C. C.P. No.1103
28th March, 1968
M.R.A. Shaalan

A WIND-TUNNEL INVESTIGATION OF THE STALLING PERFORMANCE
OF TWO COMPRESSOR CASCADES OF DIFFERENT ASPECT RATIOS
AT LOW SPEED

Two compressor cascades of aspect ratio 2.10 and 4.83 were tested up to the stall point in a working section with solid side walls. A change in aspect ratio was obtained by changing the blade chord only. The blade section profile was the 10C4/30C50, staggered at 36 degrees with a space-chord ratio of 0.88, and there was no tip clearance. Reynolds number similarity was maintained but its value was kept above a "critical" value.

The/

A.R.C. C.P. No.1103
28th March, 1968
M.R.A. Shaalan

A WIND-TUNNEL INVESTIGATION OF THE STALLING PERFORMANCE
OF TWO COMPRESSOR CASCADES OF DIFFERENT ASPECT RATIOS
AT LOW SPEED

Two compressor cascades of aspect ratio 2.10 and 4.83 were tested up to the stall point in a working section with solid side walls. A change in aspect ratio was obtained by changing the blade chord only. The blade section profile was the 10C4/30C50, staggered at 36 degrees with a space-chord ratio of 0.88, and there was no tip clearance. Reynolds number similarity was maintained but its value was kept above a "critical" value.

The/

The high aspect ratio blade gave more deflection at mid-span near stall, but it stalled earlier and suddenly. The low aspect ratio blade stalled more progressively. High pressure rise coefficient is observed at the high aspect ratio, increasing slightly with incidence up to the stall point. The increase in axial velocity for both cascades was remarkably high, a greater spanwise contraction being evident for the low aspect ratio.

Area traverses downstream showed that the wall stall for the high aspect ratio blade was nearly equally distributed between the blade surface and the end wall, whilst for the low aspect ratio blade it was shifted towards the blade surface.

The high aspect ratio blade gave more deflection at mid-span near stall, but it stalled earlier and suddenly. The low aspect ratio blade stalled more progressively. High pressure rise coefficient is observed at the high aspect ratio, increasing slightly with incidence up to the stall point. The increase in axial velocity for both cascades was remarkably high, a greater spanwise contraction being evident for the low aspect ratio.

Area traverses downstream showed that the wall stall for the high aspect ratio blade was nearly equally distributed between the blade surface and the end wall, whilst for the low aspect ratio blade it was shifted towards the blade surface.

The high aspect ratio blade gave more deflection at mid-span near stall, but it stalled earlier and suddenly. The low aspect ratio blade stalled more progressively. High pressure rise coefficient is observed at the high aspect ratio, increasing slightly with incidence up to the stall point. The increase in axial velocity for both cascades was remarkably high, a greater spanwise contraction being evident for the low aspect ratio.

Area traverses downstream showed that the wall stall for the high aspect ratio blade was nearly equally distributed between the blade surface and the end wall, whilst for the low aspect ratio blade it was shifted towards the blade surface.



C.P. No. 1103*

© *Crown copyright 1970*

Printed and published by
HER MAJESTY'S STATIONERY OFFICE

To be purchased from
49 High Holborn, London WC1
13a Castle Street, Edinburgh EH2 3AR
109 St Mary Street, Cardiff CF1 1JW
Brazennose Street, Manchester M60 8AS
50 Fairfax Street, Bristol BS1 3DE
258 Broad Street, Birmingham 1
7 Linenhall Street, Belfast BT2 8AY
or through any bookseller

Printed in England

C.P. No. 1103*

SBN 11 470343 4